LEVEL

ARL-TR-81-19

AD A101418

THEORETICAL ANALYSIS OF THE EFFECTS OF TURBULENCE ON A MOBILE PARAMETRIC RECEIVER

C. Robert Culbertson

APPLIED RESEARCH LABORATORIES
THE UNIVERSITY OF TEXAS AT AUSTIN
POST OFFICE BOX 8029, AUSTIN, TEXAS 78712

1 April 1981

Technical Report

DTIC
ELECTE
JUL 1 5 1981
S
C

Prepared for:

NAVAL SEA SYSTEMS COMMAND
DEPARTMENT OF THE NAVY
WASHINGTON, DC 20362

8

81 7 13 228

SECURITY CLASSIFICATION OF THIS PAGE *(When Data Entered)*

REPORT DOCUMENTATION PAGE		READ INSTRUCTIONS BEFORE COMPLETING FORM
1. REPORT NUMBER	2. GOVT ACCESSION NO. AD-A101418	3. RECIPIENT'S CATALOG NUMBER
4. TITLE *(and Subtitle)* THEORETICAL ANALYSIS OF THE EFFECTS OF TURBULENCE ON A MOBILE PARAMETRIC RECEIVER .		5. TYPE OF REPORT & PERIOD COVERED Technical Report.
		6. PERFORMING ORG. REPORT NUMBER ARL-TR-81-19
7. AUTHOR(s) C. Robert Culbertson		8. CONTRACT OR GRANT NUMBER(s) N00024-77-C-6200
9. PERFORMING ORGANIZATION NAME AND ADDRESS Applied Research Laboratories The University of Texas at Austin Austin, TX 78712		10. PROGRAM ELEMENT, PROJECT, TASK AREA & WORK UNIT NUMBERS Item 0011
11. CONTROLLING OFFICE NAME AND ADDRESS Naval Sea Systems Command Department of the Navy Washington, DC 20362		12. REPORT DATE 1 Apr 1981
		13. NUMBER OF PAGES 88
14. MONITORING AGENCY NAME & ADDRESS*(if different from Controlling Office)*		15. SECURITY CLASS. *(of this report)* UNCLASSIFIED
		15a. DECLASSIFICATION DOWNGRADING SCHEDULE N/A

16. DISTRIBUTION STATEMENT *(of this Report)*

Approved for public release; distribution unlimited.

JUL 15 1981

17. DISTRIBUTION STATEMENT *(of the abstract entered in Block 20, if different from Report)*

18. SUPPLEMENTARY NOTES

19. KEY WORDS *(Continue on reverse side if necessary and identify by block number)*

parametric receiver
nonlinear acoustics
turbulence

20. ABSTRACT *(Continue on reverse side if necessary and identify by block number)*
This report presents the development of analytical expressions that describe some effects of turbulence on the performance of a mobile parametric receiver. The report is organized into three general topics: (1) summaries of literature pertaining to parametric reception, turbulence, and wave propagation in inhomogeneous media; (2) theoretical analysis; (3) theoretical estimates of the effects of turbulence on parametric reception. It is concluded that turbulence can produce significant amplitude and phase fluctuations in the acoustic signal

DD FORM 1 JAN 73 1473 EDITION OF 1 NOV 65 IS OBSOLETE

20. (cont'd)

detected by the parametric receiver, but that experiments are required to
determine the level of fluctuations that might be expected in a practical
application.

Accession For

NTIS GRA&I
DTIC TAB
Unannounced
Justification

By
Distribution/

Availability

Dist

A

TABLE OF CONTENTS

iii

TABLE OF CONTENTS (Cont'd)

LIST OF FIGURES

v

I. INTRODUCTION

The parametric receiver utilizes the nonlinearity of acoustic wave propagation in water to synthesize a virtual array between two transducers, the pump and hydrophone (see Appendix A for details). This virtual array has the directivity characteristics of a conventional end-fired array of the same length as the pump-hydrophone separation, but with a considerable reduction in the number of transducers required. The main advantage of using a parametric receiver in a submarine application, therefore, is that a narrow, conical receiving beam can be obtained with minimum hardware in the water. This receiving beam has a front-to-back ratio and a vertical directivity that discriminate against noise at the mid-frequencies. Also, since the virtual array is synthesized in the water, it is reformed (or stabilized) at the speed of sound during maneuvers and heading changes. Because there are no transducer elements between pump and hydrophone, the parametric receiver may be less sensitive to flow noise as boat speed increases. These characteristics of the parametric receiver contribute to its attractiveness in submarine passive sonar applications. However, there are possible performance limitations of mobile parametric receivers that need to be considered.

Because the parametric receiver effectively forms an array in the medium between pump and hydrophone, its operation is sensitive to the state of the medium in this region. The presence of air bubbles, pieces of hardware, or significant temperature or flow velocity gradients will modify the synthesized array and alter its performance. In particular, at moderate or high boat speeds, the turbulence produced in the wake of the pump transducer may have several effects on the performance of the parametric receiver. The turbulence will act as a volume distributed, low frequency acoustic source that will increase the noise level of the parametric receiver. Turbulence will also scatter the acoustic waves

1

propagating between pump and hydrophone, thereby producing random amplitude and phase fluctuations in the detected acoustic signals. These effects of turbulence need to be investigated in order to determine the viability of the parametric receiver as a submarine passive sonar.

The objective of the present study is to analytically determine the effects of turbulence on the performance of the mobile parametric receiver, with emphasis on the effects of turbulent scattering. The study has been organized into three general areas. (1) A literature survey has been conducted in the areas of parametric reception, turbulence, and wave propagation in inhomogeneous media. Summaries of material from these areas that pertain to the study are presented in Appendices A, B, and C. (2) Theoretical expressions have been developed for the acoustic amplitude and phase fluctuations caused by turbulent scattering. A summary and discussion of this theory is presented in Section II of this report, with details of the analysis given in Appendices D and E. (3) Approximate numerical estimates of the effects of turbulence on parametric reception have been made using the developed theory. These estimates are presented and discussed in Section III of the report. Finally, in Section IV, conclusions are drawn regarding the limitations imposed by turbulence on mobile parametric reception, and future work is discussed.

2

II. THEORETICAL RESULTS

A. Introduction

Suppose a parametric receiver consisting of pump transducer and hydrophone is placed on a vessel moving from right to left through the medium. If the transducers are placed clear of the boundary layer turbulence produced by the vessel's hull, then the situation can be modeled by considering two stationary transducers in a fluid that flows from left to right, as shown in Fig. 1. The flow will separate in the region of the pump transducer, and vortices will form. At some distance downstream from the transducer, the vortices will decompose into the random velocity field that characterizes turbulence. The dimensions and intensity of the turbulence are dependent upon the flow velocity and upon the geometry of the rigid boundaries associated with the flow.

As shown in Appendix B, the eddies associated with turbulent flow may be treated as "patches" of variable refractive index. These patches, or inhomogeneities, will scatter the acoustic waves propagating in the interaction region between pump transducer and hydrophone. As a result of scattering, amplitude and phase fluctuations in both pump and sideband waves will occur (see Appendix C).

The fluctuations in the sideband waves are a source of noise to the parametric receiver that can act to degrade its performance in the detection of acoustic signals. The purpose of the theoretical work discussed in this section is to obtain expressions for the amplitude and phase fluctuations in the sideband waves in terms of parameters of the turbulence.
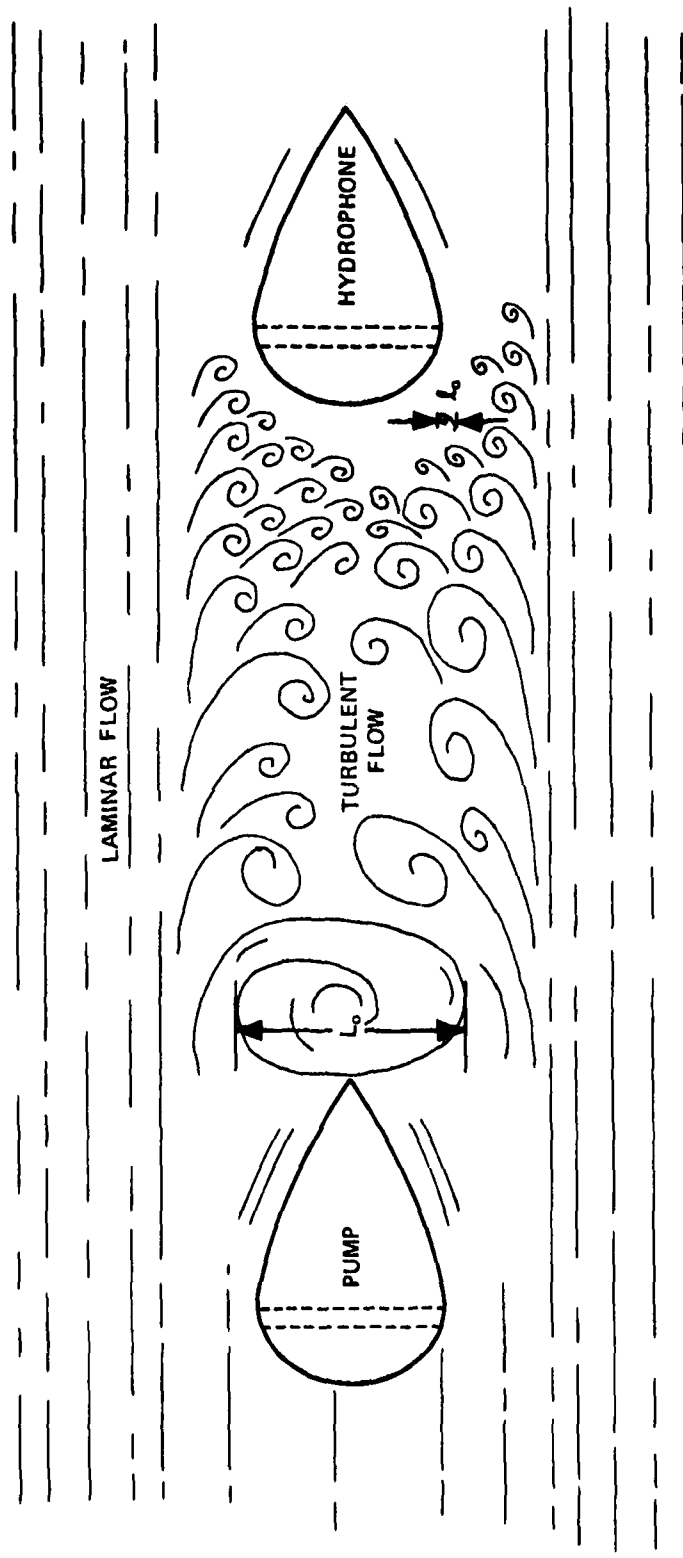
FIGURE 1
GENERATION OF TURBULENCE IN INTERACTION REGION

B.   Summary of Theoretical Analysis

1.   Analysis for Weak Turbulence

A detailed analysis of the effects of weak turbulence on the performance of a mobile parametric receiver is given in Appendix D. In this analysis, the acoustic waves are modeled as follows. The pump wave is assumed to be spherically spreading, but confined to a narrow beam by the directivity of the pump transducer. There are fluctuations B_p and S_p in the amplitude and phase, respectively, of the pump wave. For the case of weak turbulence, these fluctuations are assumed to be small (i.e., less than 10% of the mean amplitude or phase). The signal wave is assumed to be planar and, because of its relatively low frequency, is assumed to have a negligible level of fluctuations due to the turbulence in the interaction region.

The interaction of these two first-order waves (the pump and signal waves) produces an array of virtual sources in the region between pump and hydrophone. The second-order pressure radiated from each virtual source will have amplitude and phase fluctuations, $B_{\pm}$ and $S_{\pm}$, respectively, due to scattering caused by turbulence. The second-order pressure $p_{\pm}$ detected by the hydrophone of the parametric receiver will therefore depend upon the fluctuation terms B_p, S_p, $B_{\pm}$, and $S_{\pm}$.

The mean squared amplitude and phase fluctuations in the pressure $p_{\pm}$ are shown in Appendix D to be

$$<B_{PR}^2> \doteq 0.1415 \ C_n^2 \ k_p^{7/6} L^{11/6} \tag{1}$$

$$<S_{PR}^2> \doteq 0.8889 \ \sqrt{\pi} \ <\mu^2> \ k_p^2 \ aL \quad \text{for } D>>1, \text{ and} \tag{2}$$

$$<S_{PR}^2> \doteq 1.778 \ \sqrt{\pi} \ <\mu^2> \ k_p^2 \ aL \quad \text{for } D<<1 \quad ,$$

5

where

C_n is the turbulence structure constant,

k_p is the acoustic wave number at frequency ω_p,

L is the pump-hydrophone separation,

$<\mu^2>$ is the mean squared refractive index variation,

a is the mean correlation distance of the refractive index, and

$$D = \frac{4L}{ka^2} \quad .$$

Equations (1) and (2) are expressions for fluctuations in the detected pressure $p_\pm$ in terms of the acoustic wave number, the array length L, and the turbulence parameters C_n, $<\mu^2>$, and a. These results indicate that the fluctuations increase with the intensity of the turbulence in the interaction region. This is because the amplitude and phase fluctuations increase with C_n^2 and $<\mu^2>$, respectively, and both of these parameters are related to turbulent intensity. Also from Eqs. (1) and (2), it can be seen that the fluctuations increase with the separation L of the pump and hydrophone. This is reasonable, because as L increases the number of scatterers that lie in the paths of the propagating waves is increased.

Equations (1) and (2) were obtained using the assumption that complete longitudinal correlation of fluctuations exists in the interaction region of the parametric receiver. This assumption has the effect of making the equations apply for the "worst case", and thus give maximum values of fluctuations. In applications where the pump-hydrophone separation is greater than the correlation distance of the pump wave fluctuations, $<B_{PR}^2>$ and $<S_{PR}>$ will be less than values obtained from Eqs. (1) and (2). General expressions for calculating $<B_{PR}^2>$ and $<S_{PR}^2>$ are given in Appendix D [Eqs. (D-24) and (D-30)].

The results are also based on the assumption that the fluctuations in the pump and interaction frequency waves remain small. This amounts to assuming that the turbulence is sufficiently weak for given array lengths and acoustic wave numbers that small perturbation theory is applicable to the problem. For stronger turbulence, where the

methods of small perturbation theory no longer apply, it is useful to make a *simpler theoretical model than that used in Appendix D.*

2. Analysis for Strong Turbulence

It is shown in Appendix E that the fluctuations in the sideband pressure $p_\pm$ are approximately equal to corresponding fluctuations in the pump wave. In other words,

$$\langle B_{PR}^2 \rangle \doteq \langle B_p^2 \rangle \quad ,$$

and

$$\langle S_{PR}^2 \rangle \doteq \langle S_p^2 \rangle \quad .$$

As an approximate solution to the problem of strong turbulence, smooth perturbation theory for linear waves may be used to obtain the following results (see Appendix E for details):

$$\langle B_{PR}^2 \rangle \doteq 0.13 \ C_n^2 \ k_p^{7/6} \ L^{11/6} \quad , \tag{3}$$

and

$$\langle S_{PR}^2 \rangle \doteq 0.50 \ \sqrt{\pi} \ \langle \mu^2 \rangle \ k_p^2 \ aL \quad . \tag{4}$$

It can be seen that these results are approximately equal to the expressions in Eqs. (1) and (2), the difference being in the numerical constants. This difference is more severe for the phase fluctuations than for the amplitude fluctuations. However, Eqs. (3) and (4) are valid for rms fluctuation levels up to about 50%, whereas Eqs. (1) and (2) are valid only up to rms fluctuation levels of about 10%. The simple "strong turbulence" model described in Appendix E thus has the effect of extending the range of validity of the theoretical results obtained in Appendix D, although for $\langle S_{PR}^2 \rangle$ the approximation is somewhat crude.

7

III. THEORETICAL EXAMPLES

The results summarized in Section II can be used to predict rms levels of fluctuations, $<B_{PR}^2>^{1/2}$ and $<S_{PR}^2>^{1/2}$, for a mobile parametric receiver. As the theoretical results depend strongly upon parameters of turbulence, some estimates for these parameters need to be made. It is shown in Appendix F that the pertinent parameters may be calculated as follows. The structure constant C_n is given by

$$C_n^2 \doteq 8.487 \times 10^{-8} \, v^2 \, L_o^{-2/3} \quad , \tag{5}$$

where

   v is the velocity of the vessel in m/sec, and

   L_o is the outer scale of turbulence, determined by dimensions of the flow around the pump transducer housing.

The mean square refractive index variations are

$$<\mu^2> \doteq \left(0.3162 \, v/c_o\right)^2 \quad , \tag{6}$$

where c_o is the mean sound speed in m/sec. The mean correlation distance associated with the refractive index variations is given by

$$a = 4.737 \times 10^{-2} \, \sqrt{L_o} \quad . \tag{7}$$

Predictions of $<B_{PR}^2>^{1/2}$ and $<S_{PR}^2>^{1/2}$ can be made by substituting Eqs. (5)–(7) into Eqs. (1) and (4). Results of such predictions appear in Figs. 2, 3, and 4. Note that "strong turbulence theory" is used for the phase fluctuations because the fluctuation levels exceed 0.1 rad for most cases considered.

9

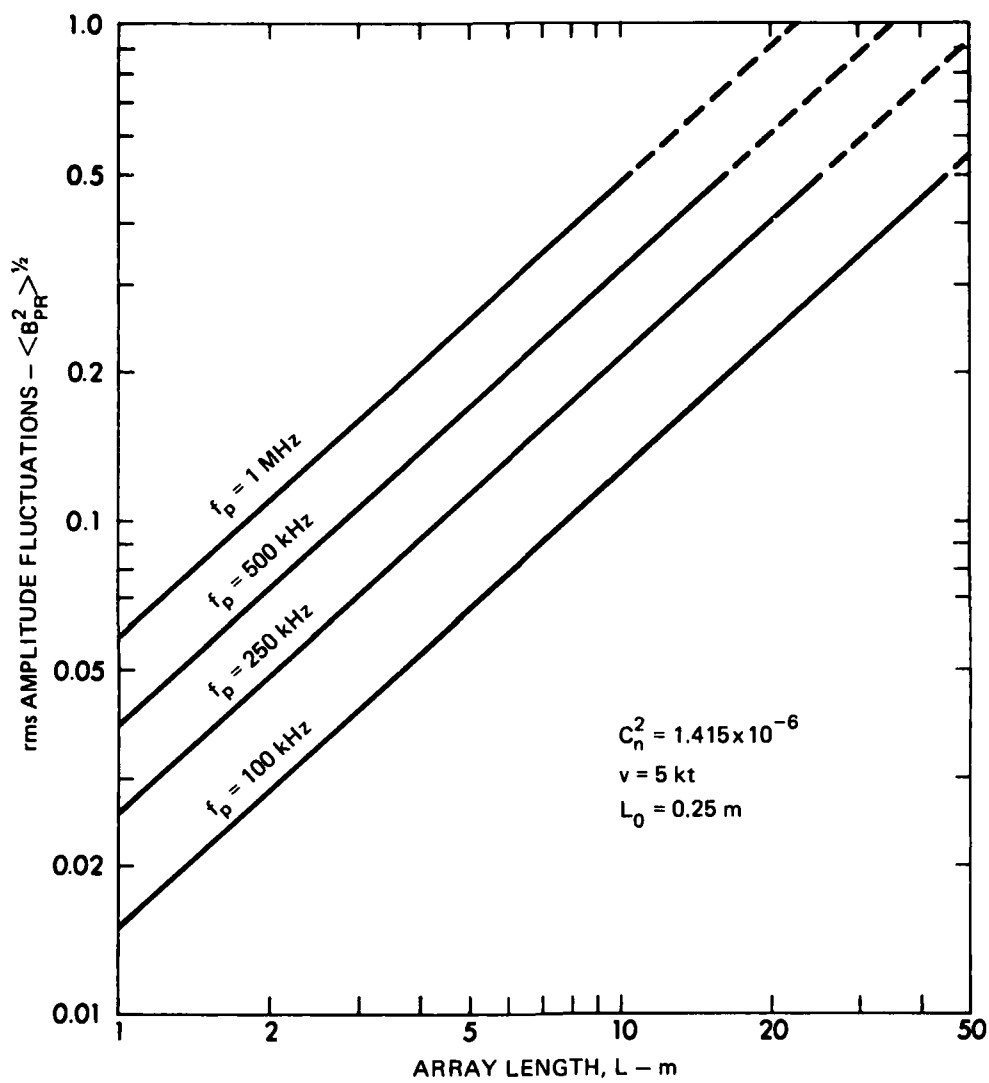**FIGURE 2**
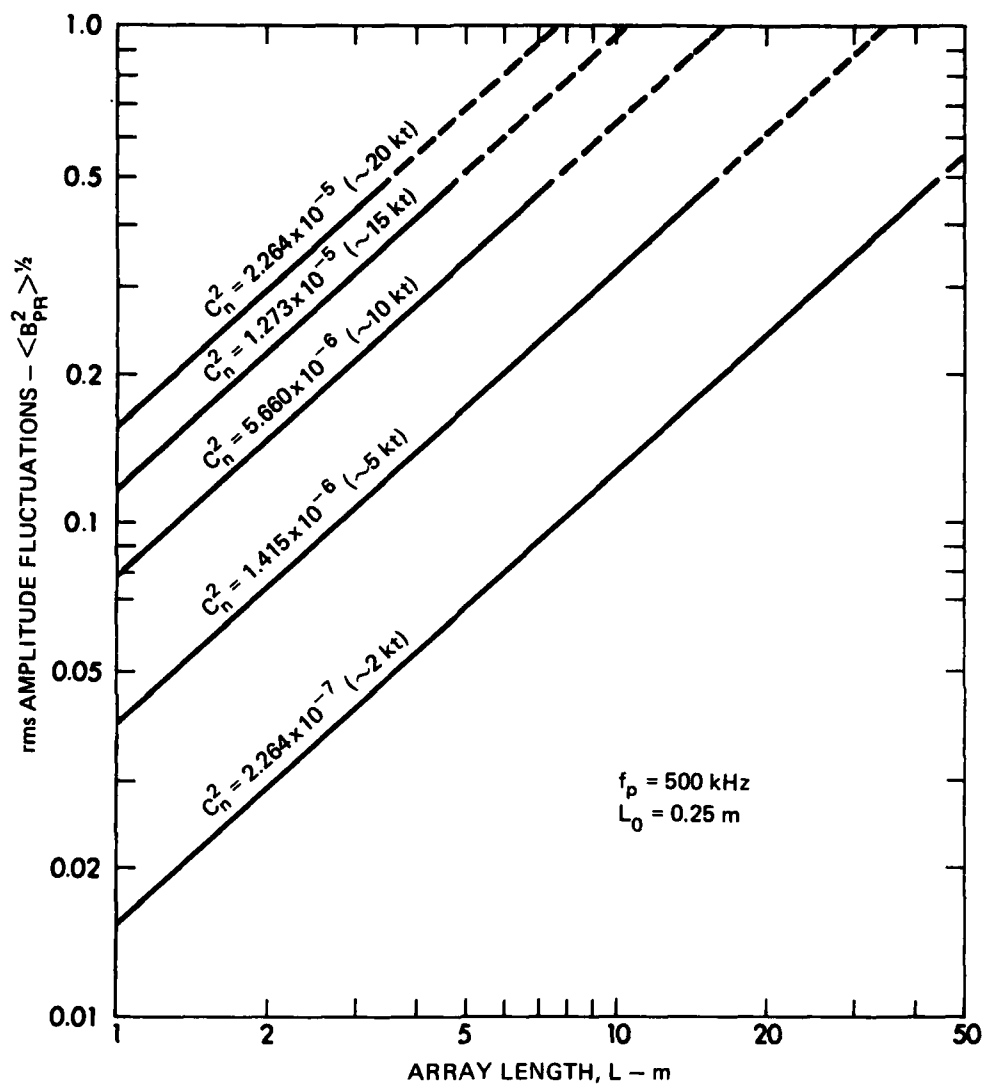**DEPENDENCE OF $\langle B_{PR}^2 \rangle^{1/2}$ UPON PUMP FREQUENCY**

FIGURE 3
DEPENDENCE OF $\langle B_{PR}^2 \rangle^{1/2}$ UPON THE STRUCTURE CONSTANT
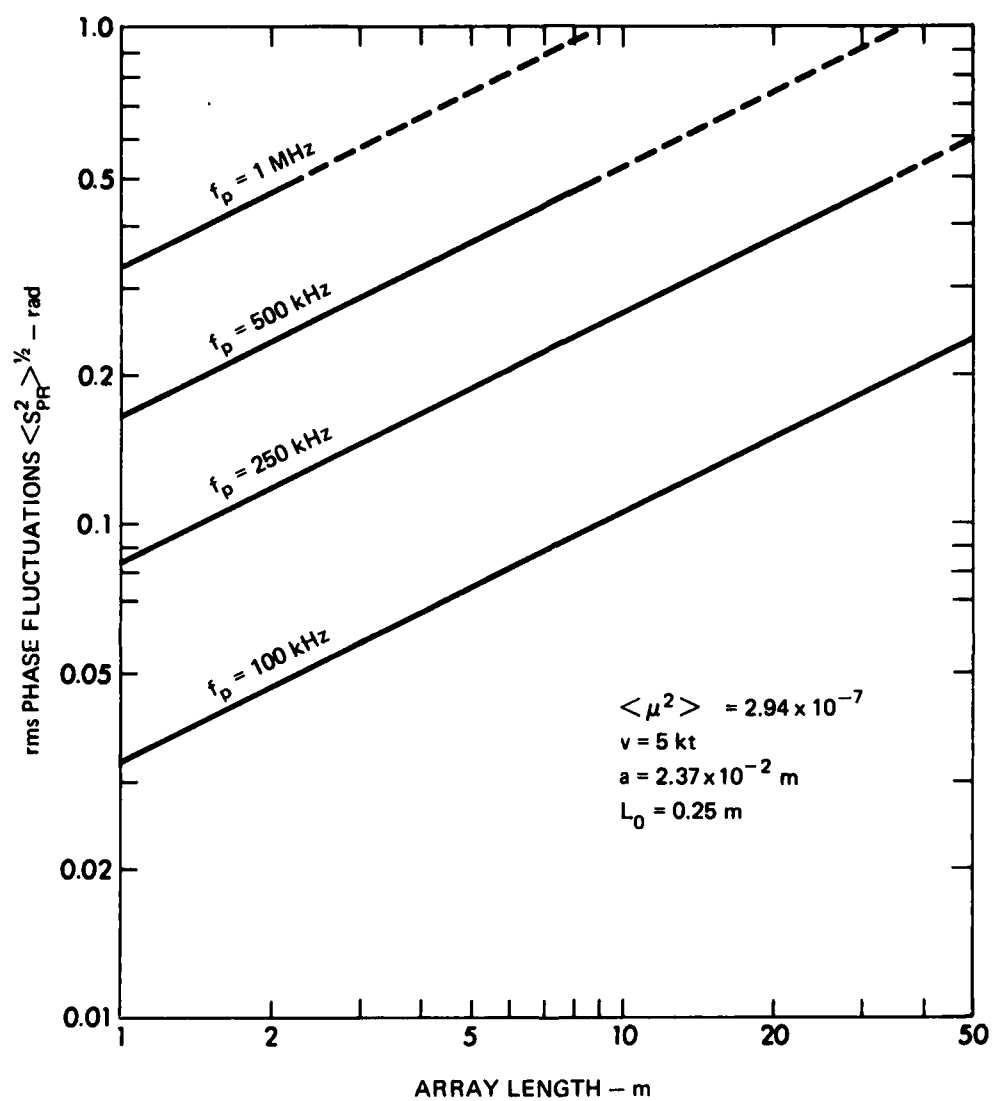
11

FIGURE 4

DEPENDENCE OF $<S^2_{PR}>^{1/2}$ UPON PUMP FREQUENCY

In Fig. 2, values of rms amplitude fluctuations $\langle B^2_{PR} \rangle^{1/2}$ are shown as a function of array length L and pump frequency f_p. These values are calculated assuming v = 5 kt and L_o = 0.25 m (here L_o is approximated as the diameter of the wake behind the pump transducer). It can be seen that, even at the low speed of 5 kt, significant levels of rms amplitude fluctuations are predicted for array lengths greater than 10 m and pump frequencies greater than 100 kHz. For example, with L = 20 m and f_p = 250 kHz, the predicted value of $\langle B^2_{PR} \rangle^{1/2}$ is approximately 0.4. This means that the "output" of the parametric receiver (i.e., the sideband pressure detected by the hydrophone) will vary in amplitude by an rms amount of 40% of its mean value. As shown in the figure, this value of fluctuation increases with increasing pump frequency.

Similar results are shown in Fig. 3 for $\langle B^2_{PR} \rangle^{1/2}$ as a function of array length L and structure constant C^2_n. Shown in parentheses are approximate values of boat speed to which the structure constants correspond. The pump frequency is assumed to be 500 kHz and L_o is again 0.25 m. It can be seen that increasing boat speed produces a significant increase in the level of amplitude fluctuation for a given array length. For an array length of 20 m, the level of amplitude fluctuation exceeds the range of validity of the theory (i.e., $\langle B^2_{PR} \rangle^{1/2}$ exceeds 0.5) for most values of C^2_n shown.

Phase fluctuations as a function of array length and pump frequency are shown in Fig. 4. These values of rms phase fluctuations $\langle S^2_{PR} \rangle^{1/2}$, in radians, are calculated for $\langle \mu^2 \rangle$ = 2.94 × 10^{-7}, which corresponds to a boat speed of approximately 5 kt, and for L_o = 0.25 m. The fluctuation levels in the figure are, for an array length of 20 m, generally in excess of 0.1. Thus it can be seen from Fig. 4 that, for pump frequencies greater than 250 kHz and array lengths greater than 20 m, the phase fluctuations will have significant levels (in excess of 0.35 radians). The levels shown in Fig. 4 may be expected to increase with boat speed in a manner similar to that demonstrated by the amplitude fluctuations. For a pump frequency of 500 kHz, $\langle S^2_{PR} \rangle^{1/2}$ will exceed 0.5 rad for speeds greater than 5 kt, even at short array lengths.

13

IV.   CONCLUSIONS AND FUTURE WORK

The objective of the investigation, to analytically determine the effects of turbulence on mobile parametric reception, has been accomplished. Theoretical expressions have been developed for the amplitude and phase fluctuations produced by turbulence in the interaction region between pump transducer and hydrophone. Predictions have been made for the level of fluctuations that can be expected in practical applications. In this section, some conclusions are drawn from the results of the investigation, and future work is discussed.

The principal conclusion that can be made is that turbulence can produce significant variations in the amplitude and phase of an acoustic signal detected by the parametric receiver. For a 20 m long parametric receiver moving at a speed of 5 kt, it has been shown theoretically that rms amplitude variations exceed 50% of the mean amplitude, and rms phase variations exceed 0.5 rad, for pump frequencies of 500 kHz and higher. It should be noted that these results are based upon the assumption of complete longitudinal correlation of both amplitude and phase fluctuations in the region between pump and hydrophone. For array lengths that are long compared to the correlation distance of the fluctuations, $<B_{PR}^2>$ and $<S_{PR}^2>$ will be less than predicted by Eqs. (1) and (2).

A second conclusion that can be drawn from the theoretical results is that the level of the fluctuations is highly dependent upon the intensity and geometry of the turbulence present in the interaction region. Specifically, $<B_{PR}^2>$ is dependent upon the structure constant C_n^2 [see Eq. (3)], and $<S_{PR}^2>$ is dependent upon the mean square refractive index variations $<\mu^2>$ and the correlation distance a.

15

This strong dependence of fluctuation levels upon the turbulence parameters means that the accuracy of any theoretical prediction of $<B_{PR}^2>$ or $<S_{PR}^2>$ is limited by the accuracy of the turbulence parameters used in making the calculation. These parameters are best determined experimentally, a point which leads to the third conclusion resulting from the investigation, that experiments are needed to determine the intensity and geometry of turbulence that can be expected in a practical application. Some data regarding these turbulence parameters should permit predictions of the effects of turbulence on mobile parametric reception that would be more accurate than those presented in Section III.

Furthermore, experimental "testing" of the assumptions made in the theoretical analysis would extend the usefulness of the present study by defining the limits of its applicability. For example, it may be found that the assumptions of isotropic turbulence and of complete transverse correlation of fluctuations are valid only for certain velocities or for certain geometrical configurations. As mentioned above, the longitudinal correlation of fluctuations in the interaction region of the parametric receiver may have great impact upon the theoretical predictions. Measurements of the longitudinal correlation coefficient for the pump wave should aid in the prediction of fluctuation levels for practical applications.

Finally, there are two effects of turbulence that have not been considered in the present study. One is the spectral broadening of the pump wave, which will contribute to the self-noise of the parametric receiver, and could reduce the minimum signal level that it can detect. A second effect is the noise generated by turbulence, both volume distributed noise and flow noise at the face of the hydrophone. This noise could also reduce the minimum detectable level of the parametric receiver. Both of these effects are more amenable to experimental than to theoretical study.

An experimental investigation generally dealing with the points discussed above has been proposed and will be sponsored by NAVSEA Code 63R, under Contract N00024-79-C-6358, Task 8.

APPENDIX A

THE PARAMETRIC ACOUSTIC RECEIVING ARRAY

The parametric acoustic receiving array (PARRAY) is an application of the parametric array, which was formulated by Westervelt[1] in 1960 and has been the subject of numerous studies[2-12] in the past two decades. Recently an integrated program[13-19] at Applied Research Laboratories, The University of Texas at Austin (ARL:UT), has demonstrated the usefulness of the PARRAY as a practical acoustic sensor.

Basic elements of the PARRAY and its operation are illustrated in Fig. A-1. The pump oscillator and power amplifier generate the high frequency continuous signal that is projected by the pump transducer. The pump wave is shown in the figure as closely spaced, concentric arcs. Ambient low frequency acoustic waves, such as the one shown by widely spaced diagonal lines, will interact nonlinearly with the pump wave to generate intermodulation products. The function of the receiver electronic hardware is to recover the information contained in the ambient signal by demodulating the interaction products, which appear as modulation sidebands on the pump carrier. Thus an ambient acoustic wave of frequency f_s produces an electrical signal at the output of the receiver electronics which also has frequency f_s.

The directional response is identical to that of a continuous, end-fired array of length L equal to the separation between pump and hydrophone. This directional response is symmetric about the line joining pump and hydrophone, so that the PARRAY forms a conical beam with half power beamwidth θ, in degrees, given approximately by

$$\theta = 105 \sqrt{\lambda/L} \quad ,$$

where λ is the acoustic wavelength of the signal to be detected.

A number of desirable characteristics result from the fact that the PARRAY is a continuous, end-fired virtual array. These characteristics[13] are summarized below.
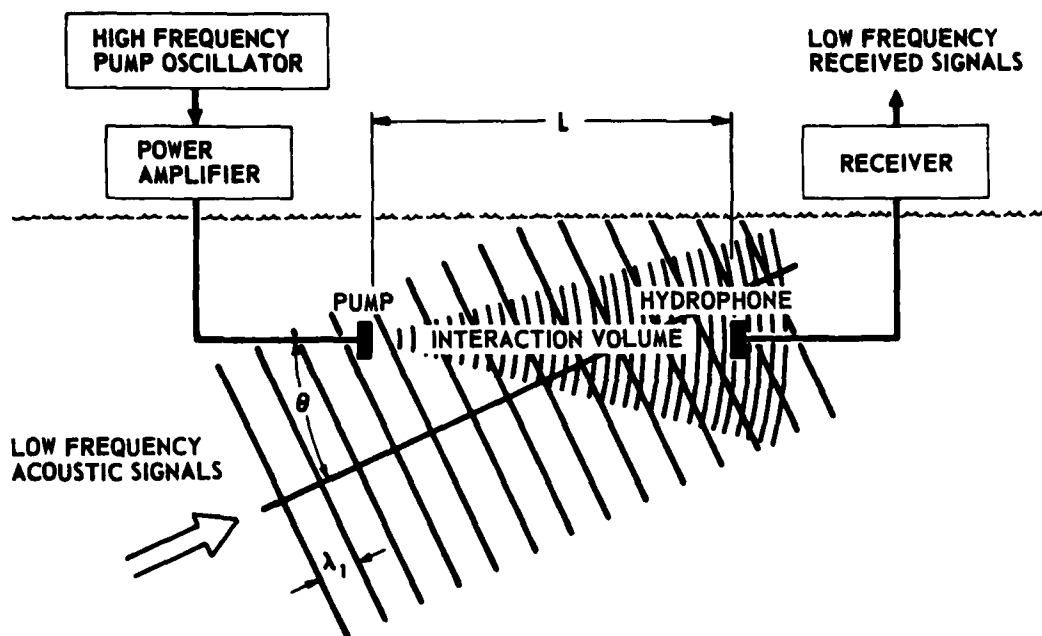
FIGURE A-1
PARRAY FUNCTIONAL DIAGRAM

20

- Vertical Directivity - Since the directional response is symmetric about the line joining the pump and hydrophone, the PARRAY provides vertical as well as horizontal discrimination against noise.

- No Grating Lobes - Grating lobes are not generated as the signal frequency increases because the PARRAY is a continuous end-fired array.

- Good Sidelobe Behavior - The sidelobes are well behaved and decrease monotonically to a minimum on the back side of the PARRAY.

- High Front-to-Back Ratio - The PARRAY is relatively insensitive to signals arriving from the back side.

- Wide Bandwidth - The PARRAY is inherently wideband because the heterodyne process translates the absolute bandwidth of the high frequency transducers to the low frequency signal region.

- Minimum Number of Transducers - Two relatively small high frequency transducers are required to form the PARRAY because the nonlinearity of the water is exploited to synthesize the array in the region between the transducers.

APPENDIX B

METHODS FOR DESCRIBING TURBULENCE

Turbulence has been the subject of extensive study since the pioneering work of Reynolds a century ago. Some excellent general references on turbulence are the books by Batchelor,[20] Hinze,[21] and Monin and Yaglom.[22] Introductory material may be found in an article by Corrsin[23] and in the books by Tennekes and Lumley[24] and by Tritton.[25] In this appendix, some basic concepts of turbulence are discussed, with emphasis on the mathematical methods used in describing turbulence.

The distinguishing feature of turbulent flow is that the fluid velocity is a random variable at any given position or time. The fluid velocity at point $\vec{r}$ and time t can be represented as the sum of mean and fluctuating components, i.e.,

$$v(\vec{r},t) = \bar{v} + v'$$

where

$\bar{v}$ is the mean velocity, and

v' is the fluctuation velocity, which is a random variable.
The "randomness" of the problem implies that it will be necessary to employ statistical parameters to describe the flow. One such description could be obtained by determining the joint probability distribution of the velocity for some number of points in the flow. This method becomes impractical if the number of points selected is large, and a simpler description is required.

Although the fluid velocity is random, it is not discontinuous, so there is some correlation between the velocity at points spaced sufficiently close together in the flow. This suggests that turbulence can be characterized by the spatial correlation coefficient,

$$R = \frac{\overline{v'(\vec{r}_1)v'(\vec{r}_2)}}{\left[\overline{v'(\vec{r}_1)^2} \; \overline{v'(\vec{r}_2)^2}\right]^{1/2}}$$

25

where the overbar denotes time averaging. The denominator of this expression is just a normalizing factor, so R basically describes the correlation of the fluctuation velocity at points $\vec{r}_1$ and $\vec{r}_2$ in the flow. If $\vec{r}_1 = \vec{r}_2$, the correlation will be maximum, and R will equal unity. As the separation between $\vec{r}_1$ and $\vec{r}_2$ increases, the correlation decreases until, at very large separations, R approaches zero. A survey of the literature related to turbulent flow[20-25] shows that the correlation coefficient just defined is one of the most frequently used parameters for describing turbulence. With small velocity probes, such as hot-wire anemometers, measurements of R in turbulent flow are often made by time averaging the velocity fluctuations at several separations $\vec{r}_2 - \vec{r}_1$.

There is another method of describing turbulence that is based upon the kinetic energy associated with the flow rather than the fluid velocity. To develop the concepts in an orderly fashion, we will need to discuss the formation of turbulent eddies.

One parameter associated with viscous fluid flow is the Reynolds number, Re, defined as

$$Re = \frac{Lv}{\nu} \quad ,$$

where

   L is the characteristic scale of flow,

   v is the characteristic flow velocity, and

   ν is the kinematic viscosity of the fluid.

For small values of Re, the fluid flow is orderly or laminar. When the Reynolds number exceeds a critical value, Re_{cr}, the flow becomes unstable and breaks up into turbulent eddies. Each eddy of size ℓ will have associated with it a local Reynolds number, Re_ℓ. If Re_ℓ also exceeds Re_{cr}, the eddy will break down further into smaller eddies. This process will continue until the eddies are small enough that viscous dissipation balances out the energy being supplied to the eddies from the external source. When this occurs, the turbulence reaches steady state, and a range of eddy sizes exists such that

26

Turbulence has been the subject of extensive study since the pioneering work of Reynolds a century ago. Some excellent general references on turbulence are the books by Batchelor,[20] Hinze,[21] and Monin and Yaglom.[22] Introductory material may be found in an article by Corrsin[23] and in the books by Tennekes and Lumley[24] and by Tritton.[25] In this appendix, some basic concepts of turbulence are discussed, with emphasis on the mathematical methods used in describing turbulence.

The distinguishing feature of turbulent flow is that the fluid velocity is a random variable at any given position or time. The fluid velocity at point $\vec{r}$ and time t can be represented as the sum of mean and fluctuating components, i.e.,

$$v(\vec{r},t) = \bar{v} + v'$$

where

$\bar{v}$ is the mean velocity, and

v' is the fluctuation velocity, which is a random variable.

The "randomness" of the problem implies that it will be necessary to employ statistical parameters to describe the flow. One such description could be obtained by determining the joint probability distribution of the velocity for some number of points in the flow. This method becomes impractical if the number of points selected is large, and a simpler description is required.

Although the fluid velocity is random, it is not discontinuous, so there is some correlation between the velocity at points spaced sufficiently close together in the flow. This suggests that turbulence can be characterized by the spatial correlation coefficient,

$$R = \frac{\overline{v'(\vec{r}_1)v'(\vec{r}_2)}}{\left[\overline{v'(\vec{r}_1)^2}\ \overline{v'(\vec{r}_2)^2}\right]^{1/2}}$$

25

$$\ell_o < \ell < L_o \quad ,$$

where

    L_o is the outer scale of turbulence, and

    ℓ_o is the inner scale of turbulence.

The outer scale L_o is determined by the boundary conditions of the fluid flow. In an acoustics application, L_o is generally taken to be the dimension from the acoustic source or receiver to the nearest boundary of the medium. The inner scale, ℓ_o, is shown by Tatarski[26,27] to be

$$\ell_o = \sqrt[4]{\nu^3/\varepsilon} \quad ,$$

where ε is the energy dissipated as heat per unit mass per unit time. We see from this expression that the inner scale of turbulence is determined by the viscosity and rate of energy dissipation in the medium, and is *independent* of the flow geometry.

In describing turbulence it is often convenient to deal with the wave number κ associated with an eddy rather than its characteristic dimension ℓ. The wave number is inversely proportional to the eddy size and may be written as

$$\kappa = \frac{2\pi}{\ell} \quad .$$

Large wave numbers correspond to small eddy sizes, and vice versa.

As discussed above, a turbulent flow with a large Reynolds number will contain a variety of eddy sizes ranging from ℓ_o to L_o. Because the kinetic energy of the flow is distributed throughout a spectrum of eddy sizes, it is possible to define a power spectral density for the flow. The average kinetic energy of the *flow* is then the sum of the energy associated with all the eddies, i.e.,[26,27]

27

$$T = \int_0^\infty \Phi_V(\kappa) d\kappa \quad ,$$

where

 T is the average kinetic energy per unit mass, and

 $\Phi_V(\kappa)$ is the power spectral density.

An example[28] of a spectrum for turbulent flow is shown in Fig. B-1. In the figure, the range of wave numbers corresponding to large, anisotropic eddies is labeled the "source" subrange, as these eddies supply energy to the entire spectrum. The energy of the source eddies gradually becomes less anisotropic (directional) in the "transitional" subrange until, in the "inertial" subrange, the energy is isotropic and homogeneous. In the inertial subrange, the spectral density is given by the simple relation[28]

$$\Phi_V(\kappa) = b\kappa^{-5/3} \quad ,$$

where b is a function of the viscosity ν and the energy dissipation rate ε. The -5/3 power law in this expression was originally proposed by Kolmogorov, and has been experimentally verified in a number of studies (e.g., see Refs. 25-28). The turbulent energy of the flow is finally lost to heat in the "dissipation" subrange, where viscous forces become dominant.

In studying waves propagating in a turbulent medium, it is useful to describe the turbulent field in terms of its refractive index. When turbulence is present in an acoustic medium, the sound speed, as a result of convection by the turbulent velocity, will be a random variable. The sound speed may then be written as

$$c = c(x,y,z,t) \quad ,$$

and the refractive index is then

28
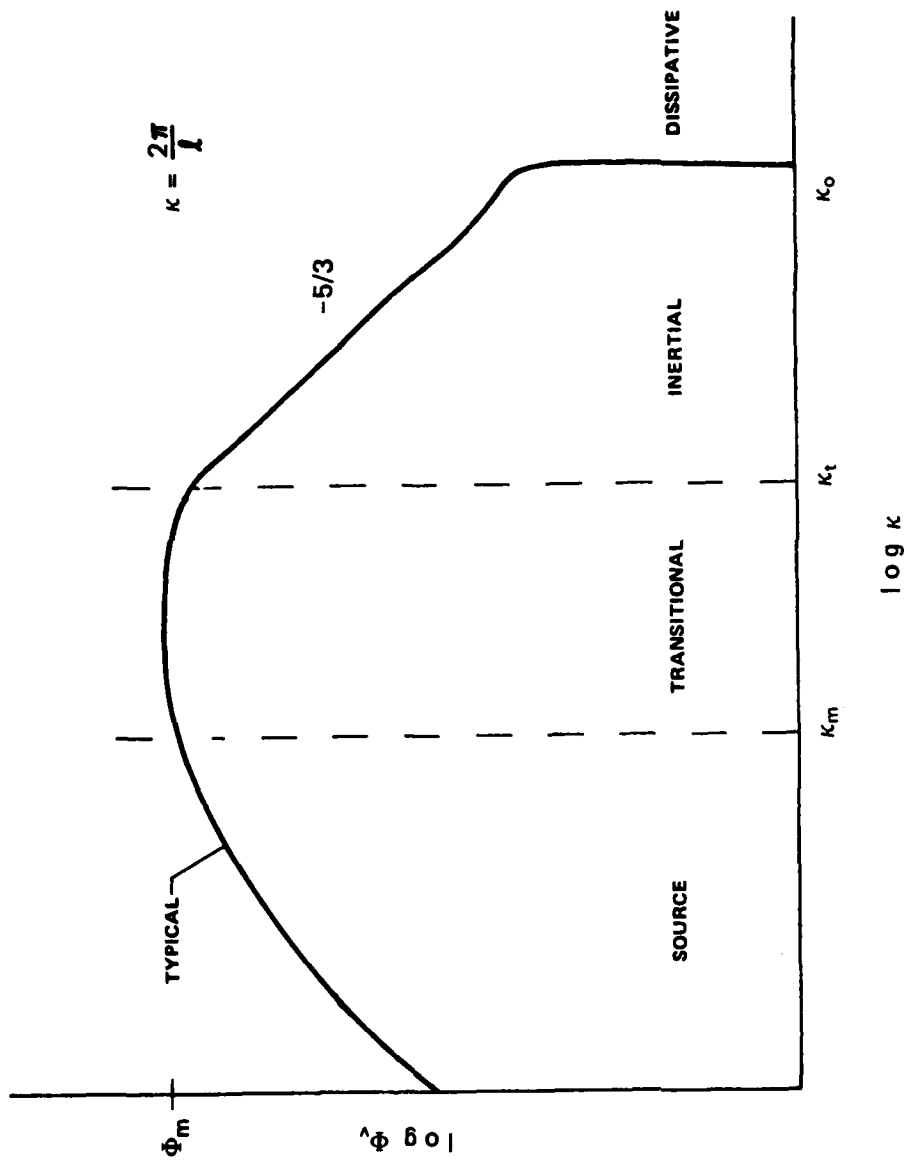
FIGURE B-1
TURBULENT POWER DENSITY SPECTRUM

29

$$n(x,y,z,t) = \frac{c_o}{c(x,y,z,t)} = 1 + \mu(x,y,z,t) \quad ,$$

where

$c_o = <c>$ is the mean sound speed,

$< >$ denotes ensemble averaging, and

$\mu(x,y,z,t)$ is the deviation from unity in the refractive index.

The two methods of representing the velocity field in turbulent flow, that of the correlation function and that of the spectral density function, can also be used to represent the refractive index field. The correlation function for the refractive index variations is defined to be[29]

$$N_{12} = \overline{\mu(\vec{r}_1,t) \; \mu(\vec{r}_2,t)} \quad .$$

If $\mu(\vec{r},t)$ is a spatially homogeneous process, then the correlation function depends only upon the separation $\Delta\vec{r}=\vec{r}_2-\vec{r}_1$.

When the separation between points becomes zero, then the correlation function has a maximum of $\overline{\mu^2}$, the mean square variation in refractive index.

If the variations in refractive index are isotropic as well as homogeneous, then the correlation function will depend only upon the magnitude of the separation between points. This condition may be written as

$$N_{12} = N_{12}(\rho) \quad ,$$

where $\rho=|\Delta\vec{r}|$. It is useful to normalize the correlation function by dividing N_{12} by $\overline{\mu^2}$. This results in the correlation coefficient R_μ, given by

$$R_\mu = N_{12} \Big/ \overline{\vec{\mu}^2} \quad .$$

A correlation coefficient frequently used to describe refractive index variations is the Gaussian function,

$$R_\mu(\rho) = \exp(-\rho^2/a^2) \quad ,$$

where a is a constant corresponding to the mean patch radius.

As in the case of the turbulent velocity field, the refractive index variations can also be described by spectral functions. These two methods of describing the random medium, that of correlation functions and that of spectral functions, are related by the Fourier transform theorem. In three dimensions, for a homogeneous medium this relation may be written as

$$N_{12}(\Delta x, \Delta y, \Delta z) = \iiint\limits_{-\infty}^{\infty} S_\mu(\kappa_1, \kappa_2, \kappa_3) \, \exp[j(\kappa_1 x + \kappa_2 y + \kappa_3 z)] d\kappa_1 d\kappa_2 d\kappa_3 \quad , \quad (B-1)$$

where

$S_\mu(\kappa_1, \kappa_2, \kappa_3)$ is the three-dimensional spectrum of the refractive index variations,

κ_1, κ_2, and κ_3 are wave numbers in the x, y, and z dimensions, respectively, and

Δx, Δy, and Δz are the x, y, and z components, respectively, of $\Delta \vec{r}$.

For an isotropic medium Eq. (B-1) becomes[28]

$$N_{12}(\rho) = \int\limits_0^{\infty} \frac{\sin\kappa\rho}{\kappa\rho} \, \Phi_\mu(\kappa) d\kappa \quad ,$$

where the one-dimensional spectral density is related to the isotropic three-dimensional spectral density by

$$\Phi_\mu(\kappa) = 4\pi\kappa^2 S_\mu(\kappa) \quad .$$

The spectrum Φ_μ of the refractive index variations will have the same shape as the velocity spectrum Φ_v,[28] so the characteristics of the subranges shown in Fig. B-1 apply to both spectra. There is an important quantity, the structure constant C_n, that can be defined for the inertial subrange of S_μ. The structure constant is a measure of the intensity of the refractive index variations, and its determination is critical when effects of turbulence on wave propagation are to be determined. In the inertial subrange, C_n is related to the spectral function S_μ by

$$S_\mu(\kappa) = 0.333 \ C_n^2 \ \kappa^{-11/3} \ , \ \kappa_t < \kappa < \kappa_o \quad .$$

In Appendix C, it will be shown that the parameters used to describe turbulence play a large role in determining the effects of turbulence on a propagating acoustic wave.

APPENDIX C

WAVE PROPAGATION IN INHOMOGENEOUS MEDIA

The effects of medium inhomogeneities on the propagation of acoustic and electromagnetic waves has received a considerable amount of study in the past three decades. In this appendix some of the basic concepts of wave propagation in inhomogeneous media are discussed, and pertinent theoretical results from the literature are summarized. Further details may be found in Refs. 26-33.

Any inhomogeneities in an acoustic medium, whether they be bubbles, biological matter, thermal patches, or turbulent eddies, may be modeled as variations in the sound velocity (or refractive index) of the medium. When there are inhomogeneities present, they scatter a propagating acoustic wave. Consequently, the total pressure at an observation point will be the sum of an unscattered pressure and a scattered pressure. Since the inhomogeneities produce the scattered pressure field, they may be treated as acoustic sources. As a first approximation, the inhomogeneities are modeled as spherical sources of radius ℓ, where ℓ is the correlation distance of the refractive index variation. If the dimensions of the inhomogeneities, or "patches," are large compared to the acoustic wavelength, the scattered sound will propagate in the same direction as the incident wave with a farfield beam angle of $1/k\ell$ radians, where k is the acoustic wave number[34] (see Fig. C-1).

The region is front of the patch out to a distance $k\ell^2$ is the nearfield or "ray region" of the scattered radiation. In this region the patch will behave like a lens, focusing or defocusing the scattered rays according to whether the sound velocity in the patch is smaller or larger, respectively, than its average value.[34] Distances from the patch farther than $k\ell^2$ are in the farfield or "wave region" of the patch.

One simple model of an inhomogenous medium is a continuous distribution of patches, each patch having radius a equal to the mean correlation distance of the refractive index variations. If an acoustic transmitter and receiver are located in such a medium, the effect that the medium has on the propagating acoustic wave will depend upon the range L_r of the receiver from the transmitter. For ranges less than ka^2, the receiver is in
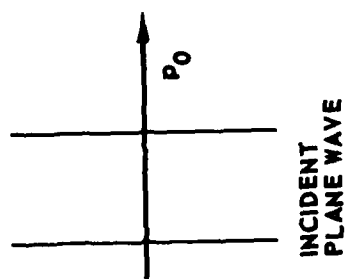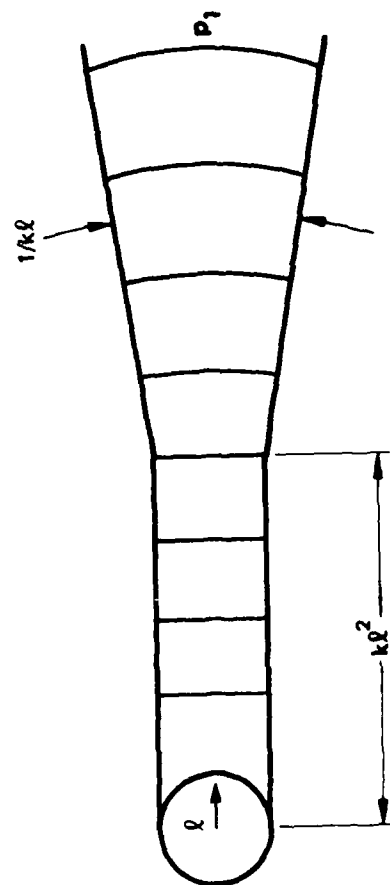
FIGURE C-1

MODELING AN INHOMOGENEITY AS A SPHERICAL SOURCE

the nearfield of patches located in the acoustic path. In this case,
effects of the inhomogeneities on the propagating wave will be largely due
to the phase delay and the focusing or defocusing that occurs as the wave
passes through the patches. The range is too short for the path differences
between the unscattered signals and the scattered signals to cause sig-
nificant diffraction effects. Conversely, for ranges $L_r >> ka^2$ the receiver
is in the farfield of most patches in the acoustic path. In this case,
interference will occur between waves scattered by various patches, and
diffraction effects will dominate. To distinguish between these two
range conditions, the wave parameter D is used, and is defined as

$$D = \frac{4L_r}{ka^2} \quad .$$

For D<<1, the receiver is in the ray region or nearfield of the patches,
and for D>>1, the receiver is in the wave region or farfield.

The main effect of medium inhomogeneities on a propagating wave is
to produce fluctuations in the wave's amplitude and phase. These fluc-
tuations occur due to the motion of the inhomogeneities, producing random
changes in the scattered pressure at the receiver. In determining the
levels of fluctuation in the received wave, only a portion of the in-
homogeneities in the medium need to be considered. For a plane wave (see
Fig. C-2(a)) only the volume contained within a cone of solid angle $1/k\ell$,
centered at the receiver, is significant.[35] Scattered pressure from
patches outside this cone does not reach the receiver. For a spherical
wave (see Fig. C-2(b)) the significant scattering volume is a narrow
ellipsoid with foci located at the transmitter and receiver.[36] This
scattering volume is approximately contained within two facing cones of
opening $1/k\ell$ centered at the projector and hydrophone.[36]

A parameter used to characterize the amplitude fluctuations of a
wave propagating through an inhomogeneous medium is the coefficient of
amplitude variation, CAV. CAV is defined as the standard deviation in
amplitude, A, of the wave, and is written as
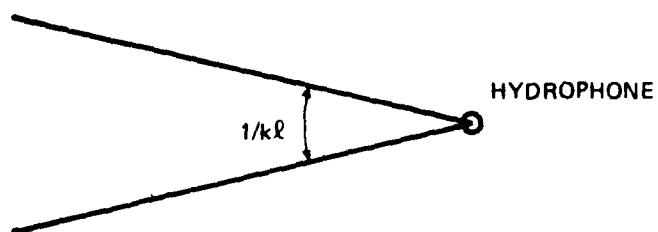
(a) FOR PLANE WAVE
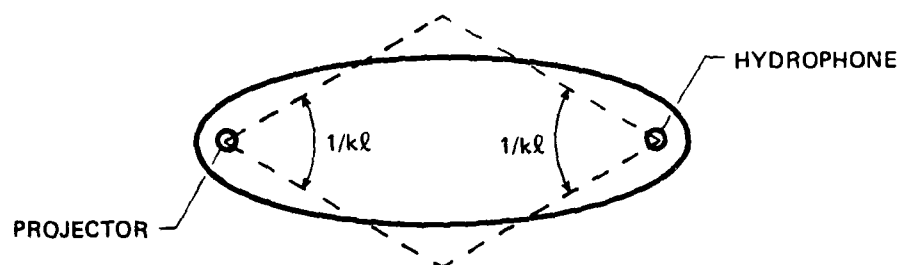
(b) FOR SPHERICAL WAVE

FIGURE C-2
SIGNIFICANT SCATTERING VOLUMES

$$CAV = \frac{(\overline{A^2} - A_o^2)^{1/2}}{A_o} \quad ,$$

where $A_o = \overline{A}$ and the overbar indicates time averaging. For mathematical reasons,[35] the log amplitude fluctuation B is often used, where B is defined as

$$B = \ln\left(\frac{A}{A_o}\right) \quad .$$

For small fluctuations,

$$B \doteq \frac{A - A_o}{A_o} \quad , \quad B \ll 1 \quad ,$$

and $\overline{B^2}$ is equivalent to CAV^2. The phase fluctuations of the wave are represented by the mean square phase deviation, where the phase deviation is

$$S = \phi - \phi_o \quad ,$$

ϕ is the instantaneous phase, and $\phi_o = \overline{\phi}$. The mean square phase deviation is therefore

$$\overline{S^2} = \overline{\phi^2} - \phi_o^2 \quad .$$

Often the ensemble averages, denoted by $<B^2>$ and $<S^2>$, are used rather than the time averages $\overline{B^2}$ and $\overline{S^2}$. For ergodic processes these two types of averages are equivalent.

Theoretical results have been obtained for the amplitude and phase fluctuations of waves propagating through a statistically isotropic

39

inhomogeneous medium. For large values of the wave parameter $(D \gg 1)$, Chernov[35] obtains

$$\langle B^2 \rangle = \langle S^2 \rangle = \langle \mu^2 \rangle \, k^2 L_r \int_0^\infty R(\rho) d\rho \quad , \quad \text{(C-1)}$$

where

μ is the deviation from unity in the refractive index n, i.e.,
$n = c_0/c = 1 + \mu$,

c_0 is the average of the sound speed, c, and

$R(\rho)$ is the correlation coefficient of the refractive index
variations.

If the correlation coefficient is Gaussian, given by $\exp(-\rho^2/a^2)$, then Eq. (C-1) becomes

$$\langle B^2 \rangle = \langle S^2 \rangle = \frac{\sqrt{\pi}}{2} \langle \mu^2 \rangle \, k^2 a L_r \quad . \quad \text{(C-2)}$$

Mintzer has shown[37,38] that Eqs. (C-1) and (C-2) are valid for a spherical wave in the wave region when

$$k^2 \langle \mu^2 \rangle a L_r \ll 1 \quad .$$

For small values of the wave parameter $(D \ll 1)$ corresponding to the ray region of the patches, Chernov shows the mean square amplitude fluctuations for a plane wave to be[35]

$$\langle B^2 \rangle = \frac{1}{6} \langle \mu^2 \rangle \, L_r^3 \int_0^\infty \nabla^2 \nabla^2 R(\rho) d\rho \quad , \quad D \ll 1 \quad , \quad \text{(C-3)}$$

which, for a Gaussian correlation coefficient, becomes

40

$$\langle B^2 \rangle = \frac{8\sqrt{\pi}}{3} \langle \mu^2 \rangle \frac{L_r^3}{a^3} \quad , \quad D \ll 1 \quad . \tag{C-4}$$

The phase fluctuations for D≪1 have been shown[35] to be twice their values when D≫1 [i.e., double the results in Eqs. (C-1) and (C-2)].

Finally, when the wave parameter is of the order of unity, Chernov obtains[35]

$$\langle B^2 \rangle = \frac{\sqrt{\pi}}{2} \langle \mu^2 \rangle \, k^2 a \, L_r \left(1 - \frac{1}{D} \arctan D \right) \quad , \tag{C-5}$$

$$\langle S^2 \rangle = \frac{\sqrt{\pi}}{2} \langle \mu^2 \rangle \, k^2 a \, L_r \left(1 + \frac{1}{D} \arctan D \right) \quad , \tag{C-6}$$

assuming a Gaussian correlation coefficient. For small and large values of D, these last two results become equivalent to the ray and wave region solutions, respectively. It is assumed in obtaining the above results that the inhomogeneities are large compared to an acoustic wavelength (ka≫1), and that the propagation distance is large compared to the scale of the inhomogeneities (L_r≫a). Using the same conditions and assumptions as Chernov, Karavainikov[36] derived a similar set of results for the amplitude and phase fluctuations in a propagating spherical wave. For the wave region of the inhomogeneities where D≫1, Karavainikov's result is identical to Eq. (C-2).

The results discussed above pertain to a medium that can be modeled as containing a continuous distribution of patches of radius a. As discussed in Appendix B, a turbulent medium contains a distribution of eddies ranging in size from the inner scale ℓ_o to the outer scale L_o. For the case of a medium whose refractive index field is determined by turbulence, techniques have been developed by Tatarski[26,27] and others[31] for calculating wave parameter fluctuations similar to the results summarized above for a Gaussian medium. In particular, Tatarski[26,27] has found expressions for amplitude fluctuations in terms of a turbulence

parameter, C_n. For propagation distances L_r such that $L_o \gg \sqrt{\lambda L_r} \gg \ell_o$, where λ is the acoustic wavelength, Tatarski shows

$$\langle B^2 \rangle \approx 0.13 \ C_n^2 \ k^{7/6} \ L_r^{11/6} \tag{C-7}$$

for spherical waves, and

$$\langle B^2 \rangle = 0.31 \ C_n^2 \ k^{7/6} \ L_r^{11/6} \tag{C-8}$$

for plane waves. The quantity C_n is related to the spectral function $S_\mu(\kappa)$ (defined in Appendix B) by[39]

$$S_\mu(\kappa) = 0.033 \ C_n^2 \ \kappa^{-11/3} \quad , \quad \kappa_t < \kappa < \kappa_p \quad .$$

An assumption made in deriving Eqs. (C-7) and (C-8) is that only the inertial range of the spectrum contributes to the acoustic fluctuations. If the spectrum is of the form shown in Fig. B-1, so that there is an approximately flat transition region, then there is an additional contribution from the transition region to the amplitude fluctuations of an amount

$$\langle B_t^2 \rangle \doteq \frac{\pi}{480} \ \Phi_m \ L_r^3 \left(\kappa_t^4 - \kappa_m^4 \right) \tag{C-9}$$

for spherical waves, and

$$\langle B_t^2 \rangle \doteq \frac{\pi}{48} \ \Phi_m \ L_r^3 \left(\kappa_t^4 - \kappa_m^4 \right) \tag{C-10}$$

for plane waves.[40] As shown in Fig. B-1, Φ_m is the maximum value of the spectral density function Φ_μ. The total mean square amplitude fluctuation, when there is a contribution due to the transition region, is $\langle B^2 \rangle + \langle B_t^2 \rangle$.

The results summarized in this appendix are used in Appendix D to obtain expressions for the amplitude and phase fluctuations in the side-band pressure of the parametric receiver.

APPENDIX D

THEORETICAL ANALYSIS OF PARAMETRIC RECEPTION
IN A TURBULENT MEDIUM

A. Introduction

The presence of turbulent eddies in the interaction region of a mobile parametric receiver will have adverse effects on receiver performance. Some effects, specifically the fluctuations in the amplitude and phase of the detected acoustic signal, are analyzed in this appendix.

The approach taken in this analysis is to treat the turbulent eddies as inhomogeneities that scatter acoustic waves propagating through the turbulence, as shown in Fig. D-1. When inhomogeneities are present in the interaction region, the virtual sources, qdv, depend not only upon the direct radiation p_p and p_s from the pump and signal sources, respectively, but also upon the scattered pump pressure, p'_p. As the scatterers move about in time, the phase difference between p_p and p'_p changes, causing amplitude and phase variations in the source density function, q. Similarly, the radiation from the virtual sources is scattered, causing further fluctuations in the amplitude and phase of the sideband signals detected by the hydrophone.

B. The Second-Order Pressure at the Hydrophone

The first major step in the analysis is to develop an expression for the second-order pressure field produced by nonlinear interaction of the pump and signal waves. This can be done by accounting for the fluctuations in the pump and signal wave that are produced by turbulence, and then calculating the Westervelt source density function.

The variations in the amplitude and phase of the pump wave are taken into account by writing

$$p_p = j(\hat{P}_p/r)\, D(\gamma)(1+B_p)\, e^{-\alpha_p r}\, e^{j(\omega_p t - k_p r - S_p)} \quad , \quad \text{(D-1)}$$
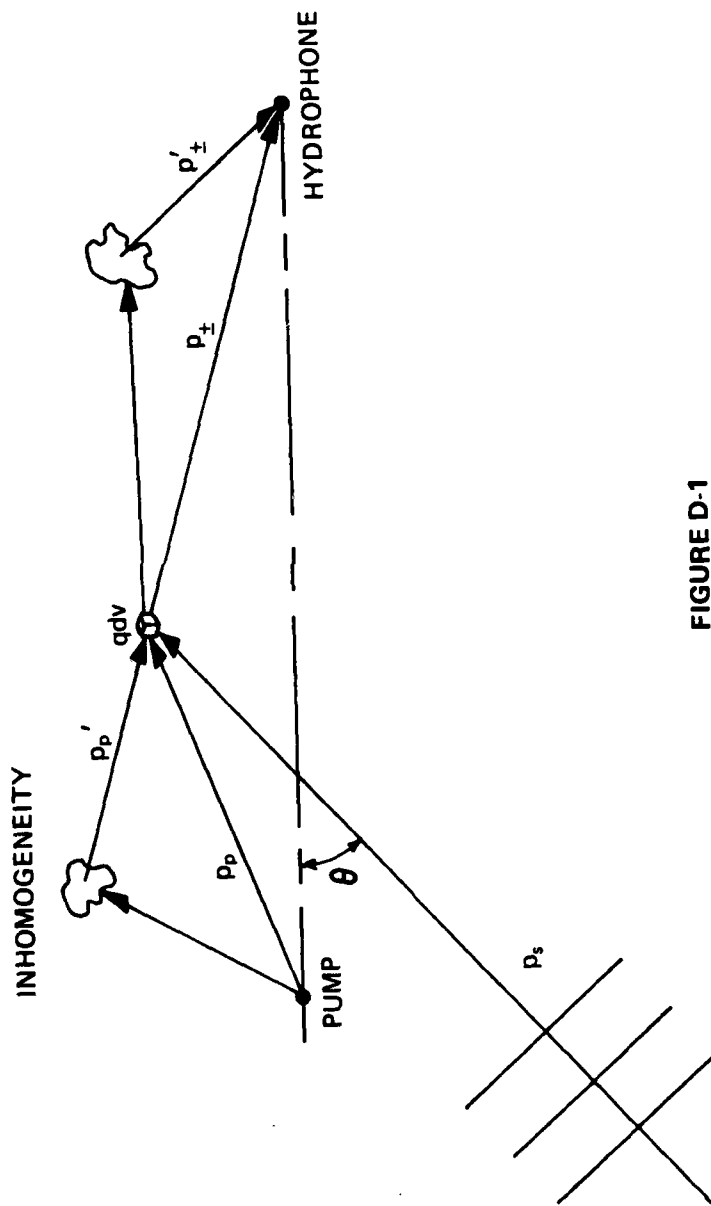
**FIGURE D-1
SCATTERING GEOMETRY**

where

$\hat{P}_p$ is the mean pump pressure amplitude at $\gamma=0$, $r=1$ m,

$D(\gamma)$ is the directivity function for the pump transducer,

$B_p = [P_p(t)-\hat{P}_p]/\hat{P}_p$ is the fractional variation of the instantaneous pressure amplitude $P_p(t)$ from its mean value, and

$S_p = \phi(t)-\overline{\phi(t)}$ is the variation of the instaneous phase $\phi(t)$ of the pump wave from its mean value, $\overline{\phi(t)}$.

The remainder of the expression represents a spherical wave propagating radially outward from an origin situated at the pump (see Fig. D-2), with angular frequency ω_p, wave number k_p, and attenuation coefficient α_p.

Inclusion of the attenuation coefficient as a constant requires that the time variations in amplitude and phase are slow compared to the pump frequency. In other words, frequency broadening of the pump wave due to the fluctuations is small enough that the attenuation coefficient remains constant.

Scattering of the signal wave in the interaction region is assumed to be negligible compared to scattering of the pump wave because of the difference in frequency of the two waves. The signal wave is therefore modeled as a plane wave having frequency ω_s, wave number k_s, and attenuation coefficient α_s:

$$P_s = P_s \, e^{-\alpha_s z} \, e^{j(\omega_s t - k_s z)} \, , \qquad (D-2)$$

where P_s is the pressure amplitude, a constant. It has been assumed for convenience that the acoustic source generating p_s is located on the maximum response axis of the parametric receiver, as shown in Fig. D-2. The signal source is assumed to be sufficiently far from the pump transducer that the signal wave is approximately planar in the vicinity of the parametric receiver.

The source density for the second-order radiation can be found using the equation

49
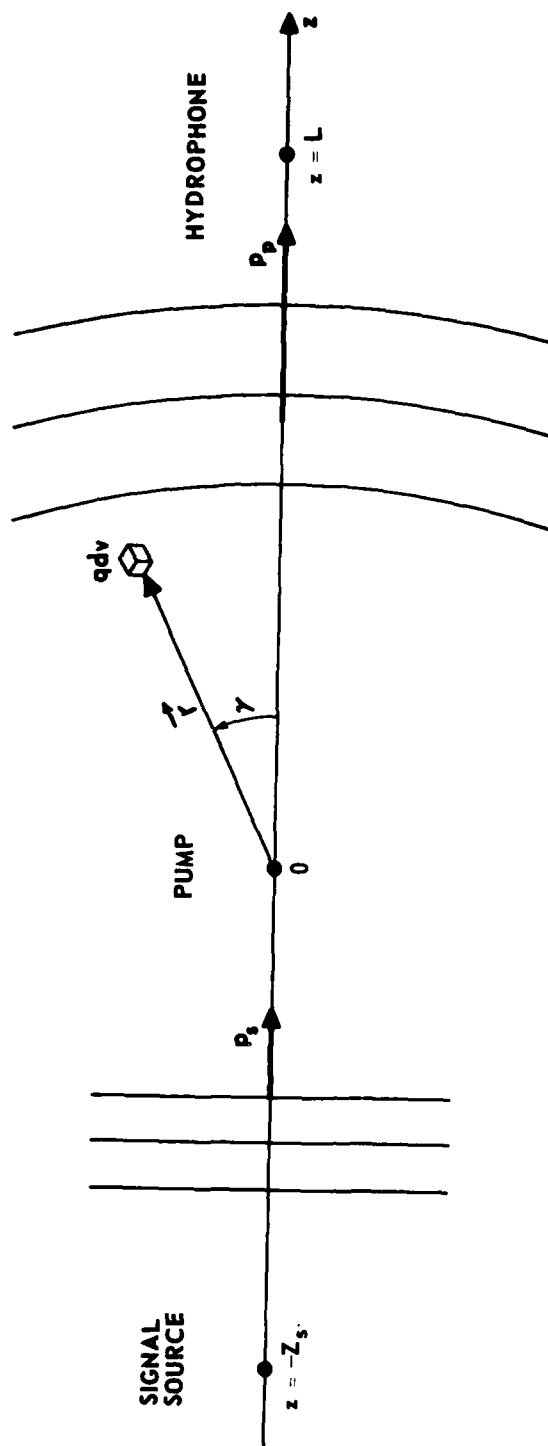
FIGURE D-2
GEOMETRY FOR ANALYZING PARRAY

$$q(\vec{r},t) = \frac{\beta}{\rho_o^2 c_o^4} \frac{\partial}{\partial t} [P_1(\vec{r},t)^2] \quad , \tag{D-3}$$

where

$\vec{r}$ is the position vector of a source point, as shown in Fig. D-2,

β is a parameter of nonlinearity,

ρ_o is the ambient density,

c_o is the ambient sound speed, and

$P_1 = P_p + P_s$ is the total first-order pressure field.

Substitution of Eqs. (D-1) and (D-2) for the total first-order pressure in Eq. (D-3) gives the source density function as

$$q = \frac{-\beta P_s \hat{P}_p \omega_\pm}{\rho_o^2 c_o^4 r} \; e^{-\alpha_s z} \; e^{-\alpha_p r} \; D(\gamma) \; (1+B_p) \; e^{-jS_p} \; e^{-j(k_p r \pm k_s z)} \; e^{j\omega_\pm t} \quad , \tag{D-4}$$

where

$\omega_\pm = \omega_p \pm \omega_s$, and

$r = |\vec{r}|$.

It is assumed that the pump wave fluctuation terms B_p and S_p have complete spatial correlation along the spherical wave fronts within the pump beam, so that B_p and S_p are independent of γ. With this assumption, a solution for the second-order pressure at the hydrophone can be obtained by adopting a procedure developed by Berktay and Shooter.[9] They assume that the sphericity of the pump wave within the beam is small compared to the wavelength at the signal frequency so that, when the signal source is collinear with the pump and hydrophone, the virtual sources $q_\pm dv$ can be assumed to be cophasal on the spherical wave fronts. The frequency of the second-order radiation is nearly equal to the pump frequency, so the second-order waves will radiate spherically, with the same beam pattern as for the pump wave. These assumptions are used to calculate the second-order pressure at the observer as follows.

51

The elemental particle velocity at r due to a spherical shell of sources of thickness δr is

$$\delta u_r = \frac{1}{2} q(r) \delta r \quad ,$$

where the source density function is given by Eq. (D-4). The contribution of these sources to the particle velocity at (L,0) will be

$$\delta u_L = (r/L)\delta u_r (1+B_u) e^{-jS_u} \exp[-(\alpha_\pm + jk_\pm)(L-r)] \quad ,$$

where

$B_u = \dfrac{U(t) \; \overline{-U(t)}}{U(t)}$ is the amplitude fluctuation,

$S_u = \phi_u(t) - k_\pm r$ is the phase fluctuation,

$U(t)$ and $\phi_u(t)$ are the amplitude and phase of the particle velocity, respectively,

$k_\pm$ is the acoustic wave number at frequency $\omega_\pm$, and

$\alpha_\pm$ is the attenuation coefficient at frequency $\omega_\pm$.

It is assumed that frequency broadening of the interaction frequency wave due to the inhomogeneities is small enough that $\alpha_\pm$ remains constant. The total particle velocity at (L,0) is the sum of contributions from all sources in the interaction region, i.e.,

$$U_\pm(L,0) = (2L)^{-1} \exp[-(\alpha_\pm + jk_\pm)L] \int_0^L (1+B_u)$$

$$\times e^{-jS_u} q(r) r \exp[(\alpha_\pm + jk_\pm)r] dr \quad . \quad \text{(D-5)}$$

The second-order pressure at the point (L,0) can now be found by using the farfield relation, $p = \rho_o cu$, in connection with Eq. (D-5). The result is

$$p_{\pm}(L,0) = \frac{-\beta P_s \hat{P}_p \omega_{\pm}}{2\rho_o c_o^3 L} \exp[-(\alpha_{\pm}+jk_{\pm})L]$$

$$\times \int_o^L (1+B_p)\,(1+B_{\pm})\,e^{-j(S_p+S_{\pm})}$$

$$\times \exp[-(\alpha_s+\alpha_p-\alpha_{\pm})z]dz \quad , \quad (D-6)$$

where $B_{\pm}$ and $S_{\pm}$ are amplitude and phase fluctuations, respectively, for the interaction frequency pressure wave. (It may be shown that the amplitude fluctuations in the pressure and particle velocity are equal; i.e., $B_u=B_{\pm}$. Similarly, $S_u=S_{\pm}$.) Since the second-order radiation is cophasal along the spherical wave fronts, a change of variable from r to z has been made in Eq. (D-6). The physical interpretation of this result follows. Nonlinear interaction of the pump and signal waves (p_p and p_s) will produce at the hydrophone of the parametric receiver a pressure wave $p_{\pm}$. The amplitude of $p_{\pm}$ increases linearly with the parameter of non-linearity, the signal and pump pressure amplitudes, and the sideband frequency. Although the array length L appears in the denominator of Eq. (D-6), some care is needed in interpreting the dependence of $p_{\pm}$ upon L. In a homogeneous medium the fluctuation terms become zero, and since

$$\alpha_{\pm} \doteq \alpha_s + \alpha_p \quad ,$$

the integral has a value L which cancels with the L in the denominator of Eq. (D-6). Thus, in the homogeneous case the amplitude of $p_{\pm}$ is independent of array length. When inhomogeneities are present, both amplitude and phase of $p_{\pm}$ depend upon fluctuations caused by turbulent scattering in the interaction region between pump and hydrophone. Ignoring attenuation, the integral in Eq. (D-6) represents the sum of the amplitude and phase fluctuations associated with each elemental length dz of the parametric receiver.

53

C. Fluctuations in the Second-Order Pressure

Now that an expression has been obtained for the second-order pressure $p_\pm$ in a turbulent medium, the next step of the analysis is to find the level of amplitude and phase fluctuations in this second-order pressure. This can be accomplished as follows.

In addition to Eq. (D-6), the sideband pressure can be written explicitly in terms of the amplitude and phase fluctuations observed at the hydrophone. If p_h is the sideband pressure that would be observed in a homogeneous medium (i.e., with no turbulence), then the sideband pressure in the presence of inhomogeneities is

$$p_\pm = p_h (1 + B_{PR}) \, e^{-j S_{PR}} \quad , \qquad (D-7)$$

where B_{PR} and S_{PR} account for the total amplitude and phase fluctuations in the sideband pressure at the hydrophone.

A solution for the amplitude and phase fluctuations B_{PR} and S_{PR} can be obtained as follows. As a first approximation, it is assumed that the acoustic wave fluctuations are sufficiently small that

$$B_p \ll 1, \qquad\qquad\qquad S_p \ll 1$$

$$B_\pm \ll 1, \qquad\qquad\qquad S_\pm \ll 1.$$

Then the amplitude fluctuation terms can be expanded and, retaining only the first-order fluctuations terms,

$$(1 + B_p)(1 + B_\pm) \doteq 1 + B_p + B_\pm \quad . \qquad (D-8)$$

Similarly, the phase fluctuations can be approximated as

$$e^{-j(S_p+S_\pm)} \doteq 1 - j(S_p+S_\pm) \quad . \tag{D-9}$$

Using Eqs. (D-8) and (D-9) for the fluctuation terms, Eqs. (D-6) and (D-7) may be set equal, giving

$$p_h(1+B_{PR}) \ e^{-jS_{PR}} \doteq A \int_o^L (1+B_p+B_\pm)[1 - j(S_p+S_\pm)]dz \quad , \tag{D-10}$$

where

$$A = \frac{-\beta P_s \hat{P}_p \omega_\pm}{2\rho_o c_o^3 L} \ e^{-(\alpha_\pm+jk_\pm)L} \quad ,$$

and the attenuation terms in the integrand of Eq. (D-6) have been approximated as

$$\alpha_s + \alpha_p - \alpha_\pm \doteq 0 \quad .$$

If the fluctuations in the sideband pressure are also assumed to be small, then

$$(1+B_{PR}) \ e^{-jS_{PR}} \doteq (1+B_{PR})(1-jS_{PR}) \quad .$$

Using this approximation and retaining fluctuation terms to first order only, Eq. (D-10) becomes

$$p_h(1+B_{PR}-jS_{PR}) = A \int_o^L (1+B-jS)dz \quad , \tag{D-11}$$

where

$$B = B_p + B_\pm, \text{ and}$$
$$S = S_p + S_\pm.$$

Subtraction of

$$P_h = A \int_0^L dz = AL$$

from both sides of Eq. (D-11) leaves

$$B_{PR} - jS_{PR} = \frac{1}{L} \int_0^L (B-jS)dz \qquad .$$

Equating real and imaginary parts of this result gives

$$B_{PR} = \frac{1}{L} \int_0^L B \ dz \qquad ,$$

and

$$S_{PR} = \frac{1}{L} \int_0^L S \ dz \qquad .$$

As B_{PR} and S_{PR} are random quantities with zero mean, it is useful to deal with the mean squared amplitude and phase fluctuations,

$$<B_{PR}^2> = \frac{1}{L^2} \int_0^L \int_0^L <B_1 B_2> \ dz_1 dz_2 \qquad , \qquad (D-12)$$

56

and

$$\langle S_{PR}^2 \rangle = \frac{1}{L^2} \int_o^L \int_o^L \langle S_1 S_2 \rangle \, dz_1 dz_2 \quad , \qquad \text{(D-13)}$$

where the angular brackets <> denote ensemble averaging. It is easier
to interpret these results physically by writing Eqs. (D-12) and (D-13)
explicitly in terms of the pump and sideband fluctuations. For example,
Eq. (D-12) can be written as

$$\langle B_{PR}^2 \rangle = \frac{1}{L^2} \int_o^L \int_o^L (\langle B_{p1} B_{p2} \rangle + \langle B_{p1} B_{\pm 2} \rangle$$

$$+ \langle B_{\pm 1} B_{p2} \rangle + \langle B_{\pm 1} B_{\pm 2} \rangle) dz_1 dz_2 \quad , \qquad \text{(D-14)}$$

where

the subscript p denotes the pump wave,

the subscript ± denotes the interaction (or sideband) frequency wave
   radiated by the virtual sources, and

the subscripts 1 and 2 refer to virtual sources located at z_1 and
z_2.

The terms in the integrand of Eq. (D-14) describe the spatial correlation
of the fluctuations. For example, $\langle B_{p1} B_{p2} \rangle$ gives the correlation between
the amplitude fluctuations in the pump wave at z_1 and the amplitude fluc-
tuations in the interaction frequency wave at z_2. The equation thus
relates the amplitude fluctuations in $p_{\pm}$ at the hydrophone to the cor-
relations of fluctuations in p_p and $p_{\pm}$ in the interaction region.

D.   Approximations for the Spatial Correlation Terms

Evaluation of Eq. (D-14) requires that the correlation terms in the
integrand be expressed as functions of z_1 and z_2. These correlation

terms fall into two categories: (1) crosscorrelation between pump
amplitude fluctuations and interaction frequency amplitude fluctuations,
and (2) autocorrelation of pump and interaction frequency amplitude fluc-
tuations. These categories are discussed separately below.

(1) Crosscorrelation. The term $<B_p(z_1)B_\pm(L-z_2)>$ represents the
crosscorrelation between pump pressure amplitude fluctuations at the
point (z_1) and interaction frequency amplitude fluctuations at $(L-z_2)$.
The frequencies of the two waves are approximately equal $(\omega_p \doteq \omega_\pm)$ so
complete frequency correlation may be assumed between B_p and $B_\pm$.

The propagation paths associated with the pump and interaction
frequency waves are shown in Fig. D-3. The term $B_p(z_1)$ is due to scat-
tering of the pump wave as it propagates from the origin to $z=z_1$. The
fluctuations in the interaction frequency wave $B_\pm(L-z_2)$ are due to
scattering of the second-order radiation as it propagates from a source
at point z_2 to the hydrophone at $z=L$. Both z_1 and z_2 may vary between
0 and L, so there will be situations in which the two propagation paths
overlap $(z_1 > z_2)$ and situations in which they are separate $(z_1 < z_2)$.

An exact solution to Eq. (D-14) requires an expression for the
correlation term $<B_p B_\pm>$ for all values of z_1 and z_2, and for both near-
field and farfield receiving arrays. This is essentially a problem of
calculating the correlation of amplitude fluctuations at two receivers
when there are two sources generating separate waves. The solution to
this problem is not available in the literature, nor is it readily
obtained, but it is convenient to make the following simplified
approximation.

Two asymptotic conditions are considered, one in which the array
length L is much less than the longitudinal correlation distance l_p and
the other in which the array length is much greater than the pump cor-
relation distance. First assume that $L << l_p$. In this case the separation
between the "receivers" at z and L is less than the pump correlation
distance, so

58

PUMP   HYDROPHONE

$z = 0$ $z = z_1$ $z = z_2$ $z = L$
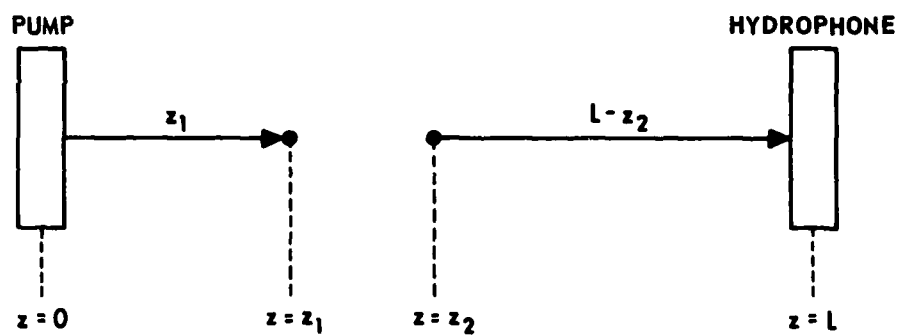
FIGURE D-3
PROPAGATION PATHS OF PUMP AND SECOND-ORDER WAVE

59

$$L - z_1 \ll 1_p \quad , \tag{D-15}$$

where 1_p is the distance at which the correlation coefficient for the pump wave amplitude fluctuations equals $1/e$. When Eq. (D-15) applies, the amplitude fluctuations of the pump wave at z_1 and the interaction frequency wave at $z=L$ will be highly correlated. Their correlation coefficient may be approximated as unity; i.e.,

$$R_{p,\pm} \approx \frac{<B_p(z_1)B_\pm(L-z_2)>}{\left[<B_p^2(z_1)><B_\pm^2(L-z_2)>\right]^{1/2}} \doteq 1 \quad , \qquad L \ll 1_p \quad .$$

From this expression the crosscorrelation between pump and interaction frequency fluctuations can be written as

$$<B_p(z_1)B_\pm(L-z_2)> \doteq \left[<B_p^2(z_1)><B_\pm^2(L-z_2)>\right]^{1/2} \quad . \tag{D-16}$$

This equation is in terms of mean square amplitude fluctuations, and can be calculated using the results discussed in Appendix C. A similar approximation can be made for the remaining crosscorrelation term in Eq. (D-14), namely

$$<B_p(z_2)B_\pm(L-z_1)> \doteq \left[<B_p^2(z_2)B_\pm^2(L-z_1)>\right]^{1/2} R_{p,\pm}$$

$$\doteq \left[<B_p^2(z_2)><B_\pm^2(L-z_1)>\right]^{1/2} \quad . \tag{D-17}$$

It should be noted that Eqs. (D-16) and (D-17) apply only for short array lengths ($L \ll 1_p$). In general, if the array length is such that $L \ll 1_p$, then $R_{p,\pm}$ is less than unity, and the following less restrictive approximations apply:

$$\langle B_p(z_2)B_\pm(L-z_1)\rangle \doteq \left[\langle B_p^2(z_2)\rangle\langle B_\pm^2(L-z_1)\rangle\right]^{1/2} R_{p,\pm} \quad , \quad \text{(D-18)}$$

and

$$\langle B_p(z_1)B_\pm(L-z_2)\rangle \doteq \left[\langle B_p^2(z_1)\rangle\langle B_\pm^2(L-z_2)\rangle\right]^{1/2} R_{p,\pm} \quad . \quad \text{(D-19)}$$

Now consider the situation when the array length is much greater than the pump longitudinal correlation distance ($L \gg l_p$). Most separations $L-z_1$ will be greater than the correlation distance l_p; therefore the fluctuations will (on the average) have very little correlation. For $L \gg l_p$ the correlation coefficient may therefore be approximated by zero:

$$\langle B_p(z_1)B_\pm(L-z_2)\rangle \doteq 0, \qquad L \gg l_p \qquad\qquad \text{(D-20)}$$

and

$$\langle B_p(z_2)B_\pm(L-z_1)\rangle \doteq 0, \qquad L \gg l_p \qquad . \qquad \text{(D-21)}$$

These results are used in Eq. (D-14) for long array lengths.

(2) <u>Autocorrelation</u>. The second category of correlation terms in Eq. (D-14) are autocorrelation functions for the pump and interaction frequency amplitude fluctuations.

The pump autocorrelation function will be given by

$$\langle B_p(z_1)B_p(z_2)\rangle = \left[\langle B_p^2(z_1)\rangle\langle B_p^2(z_2)\rangle\right]^{1/2} R_p \quad , \quad \text{(D-22)}$$

where R_p is the longitudinal correlation coefficient for pump wave fluctuations at z_1 and z_2. For short lengths ($L \ll l_p$), R_p can be approximated

as unity. For longer array lengths the results of Chernov[41] or Eliseevnin[42] can be used to estimate R_p.

The autocorrelation function for the interaction frequency wave is different from that for the pump wave. Rather than originating at a common source point and being received at different observation points, as is the pump wave, the interaction frequency waves originate at different source points and are received at a common observation point as shown in Fig. D-4. The waves originate at z_1 and z_2 and are both received at $z=L$. While there is no explicit analysis of this situation in the literature, Chotiros and Smith[40] have demonstrated that the principle of reciprocity applies as follows. If a wave of frequency $\omega_\pm$ is projected from the transducer at $z=L$, then the correlation of amplitude fluctuations received at points z_1 and z_2 will be $<B_r(L-z_1)B_r(L-z_2)>$. By the reciprocity principle, this correlation will be identical to that for waves originating at z_1 and z_2 and received at $z=L$; i.e.,

$$<B_\pm(L-z_1)B_\pm(L-z_2)> = <B_r(L-z_1)B_r(L-z_2)>   ,$$

where the subscript r indicates that the positions of sources and receivers have been interchanged. This result is useful because it leads to

$$<B_\pm(L-z_1)B_\pm(L-z_2)> = \left[<B_\pm^2(L-z_1)><B_\pm^2(L-z_2)>\right]^{1/2} R_r   ,   \text{(D-23)}$$

where R_r is the longitudinal correlation coefficient for interaction frequency waves originating at $z=L$ and received at points z_1 and z_2. When the array length is short ($L<<l_p$), the correlation coefficient is $R_r \doteq 1$. For longer array lengths, the results of Chernov[41] or Eliseevnin[42] may be used to calculate R_r. Because complete frequency correlation has been assumed for the pump and interaction frequency waves, the coefficient R_r will be equal to the longitudinal correlation coefficient for a wave at frequency ω_p received at ranges $L-z_1$ and $L-z_2$; that is,

$$R_r = R_p(L-z_1, L-z_2)   .$$

62

PUMP   HYDROPHONE

$z = 0$ z_1 z_2 $z = L$
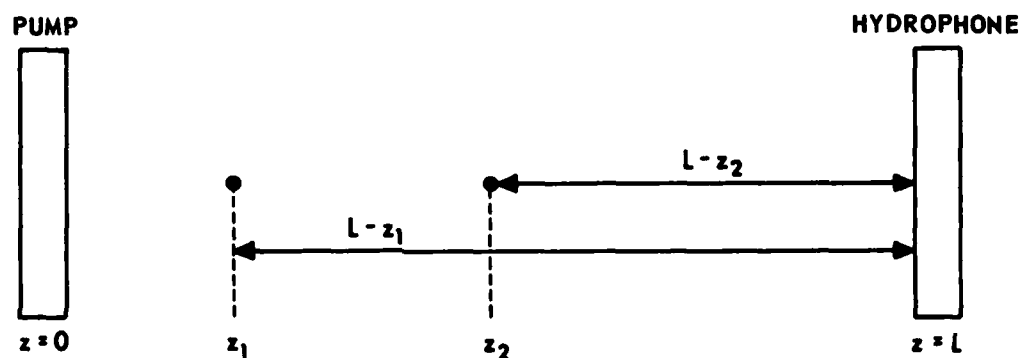
FIGURE D-4
GEOMETRY FOR AUTOCORRELATION OF
SECOND-ORDER WAVE FLUCTUATIONS

The mean squared fluctuation terms in Eq. (D-23) are for waves of frequency $\omega_\pm$ traversing paths of lengths $L-z_1$ and $L-z_2$, and may be calculated using the formulae discussed in Appendix C.

Having obtained expressions approximating the various correlation terms, it is now possible to determine the level of amplitude fluctuations produced by turbulence.

E.   Amplitude Fluctuations

The mean squared amplitude fluctuations in the second-order pressure detected by the hydrophone, $\langle B_{PR}^2 \rangle$, can now be written as

$$
\begin{aligned}
\langle B_{PR}^2 \rangle = \frac{1}{L^2} \int_0^L \int_0^L & \left\{ \left[\langle B_p^2(z_1) \rangle \langle B_p^2(z_2) \rangle \right]^{1/2} R_p + \left[\langle B_p^2(z_1) \rangle \langle B_\pm^2(L-z_2) \rangle \right]^{1/2} R_{p,\pm} \right. \\
& \left. + \left[\langle B_p^2(z_2) \rangle \langle B_\pm^2(L-z_1) \rangle \right]^{1/2} R_{p,\pm} + \left[\langle B_\pm^2(L-z_1) \rangle \langle B_\pm^2(L-z_2) \rangle \right]^{1/2} R_r \right\} dz_1, dz_2
\end{aligned} \tag{D-24}
$$

where Eqs. (D-18), (D-19), (D-22), and (D-23) have been substituted into Eq. (D-14).

As an example of evaluating Eq. (D-24), assume the array length is sufficiently short that

$$
R_p \doteq R_{p,\pm} \doteq R_r \doteq 1 \quad . \tag{D-25}
$$

If it is further assumed that

$$
L_o \gg \sqrt{\lambda_p L} \gg \ell_o \quad , \tag{D-26}
$$

so that the inertial subrange is dominating the scattering effects, then, from Eq. (C-7),

$$\langle B_p^2 \rangle = 0.13 \; C_n^2 \; k_p^{7/6} \; z^{11/6} \qquad\qquad (\text{D-27})$$

and

$$\langle B_\pm^2 \rangle = 0.13 \; C_n^2 \; k_\pm^{7/6} \; (L-z)^{11/6} \qquad . \qquad (\text{D-28})$$

Substituting Eqs. (D-27) and (D-28) into (D-24) gives

$$\langle B_{PR}^2 \rangle = \frac{0.13 \; C_n^2 \; k_p^{7/6}}{L^2} \int\!\!\int_0^L \Big[z_1^{11/12} \; z_2^{11/12} + z_1^{11/12} \; (L-z_2)^{11/12}$$

$$+ \; z_2^{11/12} \; (L-z_1)^{11/12} + (L-z_1)^{11/12} \; (L-z_2)^{11/12} \Big] dz_1, dz_2 \qquad ,$$

where it has been assumed that $k_p \doteq k_\pm$. Integration is straightforward, and the mean squared amplitude fluctuations in the second-order pressure are

$$\langle B_{PR}^2 \rangle \doteq 0.1415 \; C_n^2 \; k_p^{7/6} \; L^{11/6} \qquad . \qquad (\text{D-29})$$

This equation is one of the principal results of this analysis, for it represents the mean squared amplitude fluctuations in the "output" (upper or lower sideband pressure) of a mobile parametric receiver when turbulence is present between pump and hydrophone. The limitations imposed on this result by the assumptions used in the analysis are discussed below.

F.   Phase Fluctuations

An expression for phase fluctuations similar to Eq. (D-29) can be obtained as follows. The integral expression for the mean squared phase fluctuations, Eq. (D-13), may be expanded to give

$$\langle S^2_{PR} \rangle = \frac{1}{L^2} \iint\limits_{o}^{L} \left(\langle S_{p1} S_{p2} \rangle + \langle S_{p1} S_{\pm2} \rangle + \langle S_{\pm1} S_{p2} \rangle + \langle S_{\pm1} S_{\pm2} \rangle \right) dz_1 dz_2 \quad . \quad \text{(D-30)}$$

The spatial correlation terms in the integrand of Eq. (D-30) may be expressed in terms of parameters characterizing the turbulent medium. As discussed in Appendix C, the mean squared phase fluctuations for a wave propagating a distance L_r in an inhomogeneous medium is given by

$$\langle S^2 \rangle = \langle \mu^2 \rangle \, k^2 \, L_r \int\limits_{o}^{\infty} R(\rho) d\rho \quad , \quad \text{(C-1)}$$

where it is assumed that the wave parameter is much greater than unity (D>>1). Equation (C-1) can be used to obtain approximate expressions for the spatial correlation terms appearing in Eq. (D-30). For example, if the term $\langle S_{p1} S_{p2} \rangle$ is written in the form

$$\langle S_{p1} S_{p2} \rangle = \langle S^2_{p1} \rangle^{1/2} \langle S^2_{p2} \rangle^{1/2} R_{12} \quad ,$$

where R_{12} is the longitudinal correlation coefficient for the phase fluctuations, then Eq. (C-1) can be used to rewrite $\langle S^2_{p1} \rangle$ and $\langle S^2_{p2} \rangle$, giving

$$\langle S_{p1} S_{p2} \rangle = \left[\langle \mu^2 \rangle \, k^2_p \int\limits_{o}^{\infty} R(\rho) d\rho \right] z_1^{1/2} z_2^{1/2} R_{12} \quad . \quad \text{(D-31)}$$

If it is assumed that the correlation coefficient R_{12} is approximately unity in the interaction region of the parametric receiver, and if expressions similar to Eq. (D-31) are written for the terms $\langle S_{\pm1} S_{p2} \rangle$ and $\langle S_{\pm1} S_{\pm2} \rangle$, then Eq. (D-30) becomes

$$\langle S_{PR}^2 \rangle \doteq \langle \mu^2 \rangle \; k_p^2 \int_0^\infty R(\rho) d\rho$$

$$\times \frac{1}{L^2} \iint_0^L \left[z_1^{1/2} \; z_2^{1/2} + z_1^{1/2} (L-z_2)^{1/2} + (L-z_1)^{1/2} \; z_2^{1/2} \right.$$

$$\left. + (L-z_1)^{1/2} \; (L-z_2)^{1/2} \right] dz_1 dz_2 \quad .$$

Integration is straightforward and yields

$$\langle S_{PR}^2 \rangle \doteq 1.778 \; \langle \mu^2 \rangle \; k_p^2 \; L \int_0^\infty R(\rho) d\rho \quad .$$

Approximating the correlation term $R(\rho)$ by the Gaussian function $\exp(-\rho^2/a^2)$ gives

$$\langle S_{PR}^2 \rangle \doteq 0.8889 \; \sqrt{\pi} \; \langle \mu^2 \rangle \; k_p^2 \; aL \quad . \tag{D-32}$$

This result relates the mean squared phase fluctuations in the output of a mobile parametric receiver to the medium parameters $\langle \mu^2 \rangle$ and a. Equation (D-32) is valid only for large values of the wave parameter $(D \gg 1)$, as indicated in Eq. (C-1). For small values of the wave parameter $(D \ll 1)$, the phase fluctuations given by Eq. (C-1) increase by a factor of two,[35] and the result for $\langle S_{PR}^2 \rangle$ becomes

$$\langle S_{PR}^2 \rangle \doteq 1.778 \; \sqrt{\pi} \; \langle \mu^2 \rangle \; k_p^2 \; aL \quad . \tag{D-33}$$

G. Summary and Discussion

Theoretical analysis of parametric reception with turbulence present between pump and hydrophone has produced the following expressions for mean squared amplitude and phase fluctuations.

Amplitude Fluctuations

$$\langle B_{PR}^2 \rangle \doteq 0.1415 \ C_n^2 \ k_p^{7/6} \ L^{11/6} \tag{D-29}$$

Phase Fluctuations for D>>1

$$\langle S_{PR}^2 \rangle \doteq 0.8889 \ \sqrt{\pi} \ \langle \mu^2 \rangle \ k_p^2 \ aL \tag{D-32}$$

Phase Fluctuations for D<<1

$$\langle S_{PR}^2 \rangle \doteq 1.778 \ \sqrt{\pi} \ \langle \mu^2 \rangle \ k_p^2 \ aL \tag{D-33}$$

A number of assumptions, made in deriving these results, are summarized in Table D-1. Two assumptions, (6) and (8), are particularly important in determining the validity of the theoretical results. Assumption (6), which states that the fluctuations are small, effectively limits the levels of rms amplitude or phase fluctuations that can be predicted to approximately 10% of the mean amplitude or phase, respectively; i.e.,

$$\langle B_{PR}^2 \rangle^{1/2} \overset{\sim}{<} 0.1$$

and

$$\langle S_{PR}^2 \rangle^{1/2} \overset{\sim}{<} 0.1 \ .$$

68

TABLE D-1

LIST OF ASSUMPTIONS

1. Spherical pump wave and planar signal wave.

2. Frequency broadening of waves due to scattering is sufficiently
   small that α_s, α_p, and $\alpha_\pm$ are constants.

3. Amplitude and phase fluctuations of the signal wave are negligibly
   small.

4. There is complete correlation B_p, S_p, $B_\pm$, and $S_\pm$ along the spherical
   wave front in the interaction region.

5. Sphericity of pump wave is small enough to assume "cophasal source
   wafers" in the interaction region.

6. The scattering is sufficiently weak that B_{PR}, S_{PR}, B_p, S_p, $B_\pm$, and $S_\pm$
   remain small compared to unity.

7. $\alpha_s + \alpha_p - \alpha_\pm \doteq 0$.

8. Fluctuations B_p, S_p, $B_\pm$, and $S_\pm$ have complete longitudinal
   correlation in the interaction region ($R_p \doteq R_{p,\pm} \doteq R_r \doteq 1$).

9. Turbulence in the interaction region is homogeneous and isotropic.

In some cases of strong turbulence, high pump frequency, or long array lengths, assumption (6) may be violated, so that predicted results become inaccurate. A simple method of extending the range of validity for the theory is discussed in Appendix E.

Assumption (8), which states that the pump and interaction frequency fluctuations have complete longitudinal correlation in the interaction region, has great impact on the accuracy of the theoretical results. It can be seen from Eqs. (D-24) and (D-31) that, if these correlation terms are zero, then $<B_{PR}^2>$ and $<S_{PR}^2>$ become zero. If the correlation terms are unity, as assumed, then the results given above [Eqs. (D-29), (D-32), and (D-33)] are valid. Thus the results obtained in the previous two sections are worst-case results. If the pump and interaction frequency fluctuations are to some degree uncorrelated over the interaction region, the fluctuations $<B_{PR}^2>$ and $<S_{PR}^2>$ are reduced, and must be calculated using the general expressions in Eqs. (D-24) and (D-30). The correlation coefficients R_p, $R_{p,\pm}$, and R_r are therefore very important in determining the value of $<B_{PR}^2>$ and $<S_{PR}^2>$. Values of these correlation coefficients depend strongly upon the intensity and geometry of the turbulence present in the interaction region, and will require experimental results for accurate determinations.

APPENDIX E

EXTENSION OF RESULTS FOR STRONGER TURBULENCE

A method for obtaining approximate values of $<B_{PR}^2>$ and $<S_{PR}^2>$ for fluctuations greater than 10% of mean value is discussed in this appendix.

Comparison of Eqs. (D-27) and (D-29) shows that, for the case of weak fluctuations ($B_p <<1$ and $B_{PR} <<1$), the mean squared amplitude fluctuations in the pump and interaction frequency waves are approximately equal. In other words,

$$<B_p^2> \doteq <B_{PR}^2> \quad , \tag{E-1}$$

according to the results of the analysis in Appendix D. Similarly, using Eqs. (C-2) and (D-32),

$$<S_p^2> \doteq <S_{PR}^2> \quad , \tag{E-2}$$

although in this case the approximation is much cruder than that in Eq. (E-1).

Equations (E-1) and (E-2) form the basis of a simple theoretical model that can be used to make approximate predictions of fluctuations when the small perturbation results presented in Appendix D are no longer valid. It is assumed that the approximations in Eqs. (E-1) and (E-2) remain valid regardless of the intensity of turbulence in the interaction region. It should be noted, however, that Eqs. (D-29) and (D-32) assume that the pump fluctuations are correlated throughout the interaction region. If this assumption is violated, then approximations (E-1) and (E-2) become less accurate.

When Eqs. (E-1) and (E-2) are valid, then the determination of $<B_{PR}^2>$ and $<S_{PR}^2>$ reduces to a problem of determining the amplitude and phase fluctuations of a linear acoustic wave (the pump wave) propagating in a turbulent medium. A solution to this problem has been obtained by the method of smooth perturbation, or Rytov's method, and is available in the

73

literature.[26,27,31] Results for the amplitude and phase fluctuations are

$$<B_{PR}^2> \doteq <B_p^2> \doteq 0.13 \ C_n^2 \ k_p^{7/6} \ L^{11/6} \quad , \quad (E\text{-}3)$$

and

$$<S_{PR}^2> \doteq <S_p^2> \doteq 0.50 \ \sqrt{\pi} \ <\mu^2> \ k_p^2 \ aL. \quad (E\text{-}4)$$

Major assumptions used in deriving Eq. (E-3) are that the turbulence is isotropic and homogeneous, that the pump wave is spherically spreading, and that only the inertial subrange of the turbulence spectrum contributes to the acoustic fluctuations [see the discussion related to Eqs. (C-7)-(C-10) in Appendix C]. Equation (E-4) was derived assuming that the correlation coefficient of the refractive index variations is Gaussian and that the wave parameter D is much greater than unity [see Eq. (C-2)].

Rytov's method is valid for rms fluctuation levels up to about 0.5; i.e., the fluctuations must be such that

$$<B_{PR}^2>^{1/2} \ \tilde{<} \ 0.5 \quad ,$$

and

$$<S_{PR}^2>^{1/2} \ \tilde{<} \ 0.5 \quad .$$

APPENDIX F

TURBULENCE PARAMETERS FOR THEORETICAL EXAMPLES

In this appendix expressions are derived for the turbulence parameters that are used in calculating values of $<B_{PR}^2>^{1/2}$ and $<S_{PR}^2>^{1/2}$.

The structure constant C_n in terms of the refractive index variations and the outer scale of turbulence is given by[43]

$$C_n^2 = 1.91 \, <\mu^2> \, L_o^{-2/3} \quad , \tag{F-1}$$

where
$$\mu = -\frac{\Delta c}{c_o} \quad ,$$

Δc is the local variation in sound speed, and

L_o is the outer scale of turbulence, determined by the dimensions of the flow.

In estimating a value of μ for the turbulent wake of the pump transducer, the results given by Hinze[44] for the wake of a cylinder may be used as an approximation. For the central part of the wake, the normalized mean squared velocity fluctuations in the direction of mean flow are

$$\frac{<(\Delta v)^2>}{v^2} \doteq 0.1 \quad , \tag{F-2}$$

where v is the maximum velocity behind the obstacle in the direction of flow. Rearranging Eq. (F-2) gives

$$<(\Delta v)^2>^{1/2} \doteq \sqrt{0.1} \, v \doteq 0.3162 \, v \quad . \tag{F-3}$$

Because Δv is in the direction of the pump wave propagation, the local sound speed is increased by an amount

$$<(\Delta c)^2> = <(\Delta v)^2> \quad , \tag{F-4}$$

assuming that convection is the only mechanism contributing to a change of sound speed in the wake. Using Eqs. (F-3) and (F-4), the mean squared refractive index variations are

77

$$\langle \mu^2 \rangle = \frac{\langle (\Delta v)^2 \rangle}{c_o^2} = \left(\frac{0.3162 \ v}{c_o} \right)^2 \quad . \tag{F-5}$$

If the mean sound speed is approximately equal to 1500 m/sec, then using Eqs. (F-1) and (F-5), the structure constant may be written as

$$C_n^2 \doteq 8.487 \times 10^{-8} \ v^2 \ L_o^{-2/3} \quad .$$

Another variable that needs to be expressed in terms of the wake parameters is the refractive index correlation length a. One simple way is to assume that

$$\kappa_t = 0.5 (\kappa_p \kappa_m)^{1/2} \doteq \frac{2\pi}{a} \quad . \tag{F-6}$$

This may be interpreted physically as setting the correlation length equal to the eddy sizes that have maximum effect upon the sound propagation. This approximation is rather crude, but may be tested when measurements of turbulent flows are made. If the wave number κ_m is related to the outer scale of turbulence by

$$\kappa_m = \frac{2\pi}{\dfrac{L_o}{2}} = \frac{4\pi}{L_o} \quad , \tag{F-7}$$

then a may be found from Eqs. (F-6) and (F-7) to be

$$a \doteq 4.737 \times 10^{-2} \ \sqrt{L_o} \quad ,$$

where[40]

$$\kappa_p \doteq 5600 \ \text{m}^{-1} \ \text{at} \ 30°C \quad .$$

REFERENCES

1. P. J. Westervelt, "Parametric Acoustic Array," J. Acoust. Soc. Am. 35, 535-537 (1963).

2. H. O. Berktay, "Parametric Amplification by the Use of Acoustic Nonlinearities and Some Possible Applications," J. Sound Vib. 2, 462-470 (1965).

3. H. Date and Y. Tozuka, "Parametric Directional Microphones," Proceedings of the 6th International Congress on Acoustics, Tokyo, Japan, 21-28 August 1968.

4. H. O. Berktay and C. A. Al-Temimi, "Virtual Arrays for Underwater Reception," J. Sound Vib. 9, 295-307 (1969).

5. V. A. Zverev and Z. I. Kalachev, "Modulation of Sound by Sound in the Intersection of Sound Waves," Soviet Phys.-Acoust. 16, 204-208 (1970).

6. W. L. Konrad, R. H. Mellen, and M. B. Moffett, "Parametric Sonar Receiving Experiments," NUSC TM No. PA4-304-71, Naval Underwater Systems Center, New London, Connecticut, 9 December 1971.

7. G. R. Barnard, J. G. Willette, J. J. Truchard, and J. A. Shooter, "Parametric Acoustic Receiving Array," J. Acoust. Soc. Am. 52, 1437-1441 (1972).

8. H. O. Berktay and T. G. Muir, "Arrays of Parametric Receiving Arrays," J. Acoust. Soc. Am. 53, 1377-1383 (1973).

9. H. O. Berktay and J. A. Shooter, "Parametric Receivers with Spherically Spreading Pump Waves," J. Acoust. Soc. Am. 54, 1056-1061 (1973).

10. P. H. Rogers, A. L. Van Buren, A. O. Williams, Jr., and J. M. Barber, "Parametric Detection of Low Frequency Acoustic Waves in the Near-Field of an Arbitrary Directional Pump Transducer," J. Acoust. Soc. Am. 55, 528-534 (1974).

11. J. J. Truchard, "Parametric Acoustic Receiving Array. I. Theory," J. Acoust. Soc. Am. 58, 1141-1145 (1975).

12. J. J. Truchard, "Parametric Acoustic Receiving Array. II. Experiment," J. Acoust. Soc. Am. 58, 1146-1150 (1975).

13. Tommy G. Goldsberry et al., "Development and Evaluation of an Experimental Parametric Acoustic Receiving Array (PARRAY)," Applied Research Laboratories Technical Report No. 79-5 (ARL-TR-79-5), Applied Research Laboratories, The University of Texas at Austin, 16 February 1979.

14. Tommy G. Goldsberry, Wiley S. Olsen, C. Richard Reeves, David F. Rohde, and M. Ward Widener, "PARRAY Technology Papers Presented at Scientific and Technical Meetings," Applied Research Laboratories Technical Report No. 79-4 (ARL-TR-79-4), Applied Research Laboratories, The University of Texas at Austin, 2 August 1979.

15. D. F. Rohde, T. G. Goldsberry, W. S. Olsen, and C. R. Reeves, "Band Elimination Processor for an Experimental Parametric Acoustic Receiving Array," J. Acoust. Soc. Am. 66, 484-487 (1979).

16. Tommy G. Goldsberry, "The PARRAY as an Acoustic Sensor," Applied Research Laboratories Technical Paper No. 79-42 (ARL-TP-79-42), Proceedings of The Conference on Underwater Applications of Nonlinear Acoustics, Institute of Acoustics, The University of Bath, Bath, England, 10-11 September 1979.

17. C. Robert Culbertson, "The Parametric Receiving Array in an Inhomogeneous Medium," Applied Research Laboratories Technical Paper No. 79-69 (ARL-TP-79-69), Proceedings of the Conference on Underwater Applications of Nonlinear Acoustics, Institute of Acoustics, The University of Bath, Bath, England, 10-11 September 1979.

18. C. Robert Culbertson, "The Performance of a Parametric Receiver in an Inhomogeneous Medium," Applied Research Laboratories Technical Report No. 80-44 (ARL-TR-80-44), Applied Research Laboratories, The University of Texas at Austin, 18 August 1980.

19. D. F. Rohde, C. R. Culbertson, T. G. Goldsberry, R. A. Lamb, and C. R. Reeves, "Sea Test of a Parametric Acoustic Receiving Array at STAGE I," Final Report under Contract N00039-79-C-0209, Item 0001, Applied Research Laboratories Technical Report No. 80-37 (ARL-TR-80-37), Applied Research Laboratories, The University of Texas at Austin, 7 November 1980.

20. G. K. Batchelor, The Theory of Homogeneous Turbulence (Cambridge University Press, Cambridge, 1953).

21 J. O. Hinze, Turbulence (McGraw-Hill Book Company, Inc., New York, 1959).

22. A. S. Monin and A. M. Yaglom, Statistical Fluid Mechanics, Vols. 1 and 2 (MIT Press, Cambridge, Massachusetts, 1975).

23. S. Corrsin, "Turbulent Flow," American Scientist 49, 300-325 (1961).

24. H. Tennekes and J. O. Lumley, A First Course in Turbulence (MIT Press, Cambridge, Massachusetts, 1972).

25. D. J. Tritton, _Physical Fluid Dynamics_ (Van Nostrand Reinhold Co., New York, 1977).

26. V. I. Tatarski, _Wave Propagation in a Turbulent Medium_ (McGraw-Hill Book Company, Inc., 1961; reprinted by Dover Publications, New York, 1967).

27. V. I. Tatarski, _The Effects of the Turbulent Atmosphere on Wave Propagation_ (Published for the National Oceanic and Atmospheric Administration, U.S. Department of Commerce, and the National Science Foundation, Washington, D.C., by the Israel Program for Scientific Translations, 1971. Reproduced by National Technical Information Service, Springfield, Virginia, Document No. TT-68-50464).

28. H. Medwin, "Sound Phase and Amplitude Fluctuations due to Temperature Microstructure in the Upper Ocean," J. Acoust. Soc. Am. _56_, 1105 (1974).

29. L. Chernov, _Wave Propagation in a Random Medium_ (McGraw-Hill Book Company, Inc., 1960; reprinted by Dover Publications, New York, 1967), Chapter 1.

30. B. J. Uscinski, _The Elements of Wave Propagation in Random Media_ (McGraw-Hill International Book Company, New York, 1977).

31 A. Ishimaru, _Wave Propagation and Scattering in Random Media_, Vols. 1 and 2 (Academic Press, New York, 1977).

32 A. Ishimaru, "Theory and Application of Wave Propagation and Scattering in Random Media," Proc. IEEE _65_, 1030-1060 (1977).

33. Y. N. Barabanenkov, Y. A. Kravtsov, S. M. Rytov, and V. I. Tatarski, "Status of the Theory of Propagation of Waves in a Randomly Inhomogeneous Medium," Sov. Phys. Uspekhi _13_, 551-680 (1971).

34. E. Skudrzyk, "Scattering in an Inhomogeneous Medium," J. Acoust. Soc. Am. _29_, 50 (1957).

35. L. Chernov, _Wave Propagation in a Ran˙ Medium_ (McGraw-Hill Book Company, Inc., 1960; reprinted by ᴅᴏᵥ, ᴜblications, New York, 1967), Chapter 5.

36. V. N. Karavainikov, "Fluctuations of Amplitude and Phase in a Spherical Wave," Soviet Phys.-Acoust. 3, 175 (1957).

37. D. Mintzer, "Wave Propagation in a Randomly Inhomogeneous Medium, Part I," J. Acoust. Soc. Am. _25_, 922-927 (1953). "Part II," _25_, 1107-1111 (1953). "Part III," _26_, 186 (1954).

38. R. G. Stone and D. Mintzer, "Range Dependence of Acoustic Fluctuations in a Randomly Inhomogeneous Medium," J. Acoust. Soc. Am. _34_, 647 (1962).

39. N. P. Chotiros, "The Parametric Array in an Inhomogeneous Medium," MScQ Thesis, Dept. of Electronic and Electrical Engineering, The University of Birmingham, 1978, Equation (3.1.11).

40. N. P. Chotiros and B. V. Smith, "Sound Amplitude Fluctuations Due to a Temperature Microstructure," J. Sound Vib. <u>64</u>, 349-369 (1979).

41. L. Chernov, <u>Wave Propagation in a Random Medium</u> (McGraw-Hill Book Company, Inc., 1960; reprinted by Dover Publications, New York, 1967), Chapter 6.

42. V. A. Eliseevnin, "Longitudinal Frequency Correlation of Fluctuations of the Parameters of Plane Waves Propagating in a Turbulent Medium," Sov. Phys.-Acoust. <u>19</u>, 533-538 (1974).

43. A. Ishimaru, <u>Wave Propagation and Scattering in Random Media</u>, Vol. 2, (Academic Press, New York, 1977), p. 543.

44. J. O. Hinze, <u>Turbulence</u> (McGraw-Hill Book Company, Inc., New York, 1959), Chapter 6, Section 6.6.

DISTRIBUTION LIST FOR
ARL-TR-81-19
UNDER CONTRACT N00024-77-C-6200, ITEM 0011

Copy No.

Commander
Naval Sea Systems Command
Department of the Navy
Washington, DC 20362
1   Attn: C. D. Smith (Code 06R/63R)
2   E. Liszka (Code 63R)
3   D. E. Porter (Code 63R)
4   CAPT R. H. Scales (PMS 402)
5   D. L. Baird (Code 63X3)
6   D. M. Early (Code 63D)
7   J. Neely (Code 63X3)

Commander
Naval Electronic Systems Command
Department of the Navy
Washington, DC 20360
8   Attn: CAPT H. Cox (PME 124)
9   J. A. Sinsky (Code 320A)

Defense Advanced Research Projects Agency
1400 Wilson Boulevard
Arlington, VA 22209
10   Attn: CDR V. P. Simmons (TTO)
11   T. Kooij

Director
Naval Research Laboratory
Washington, DC 20375
12   Attn: M. Potosky (Code 5109)
13   J. Jarzinski (Code 5131)
14   R. D. Corsaro (Code 5131)

Naval Research Laboratory
Underwater Sound Reference Division
P. O. Box 8337
Orlando, FL 32856
15   Attn: J. E. Blue
16   L. Van Buren
17   P. H. Rogers

Distribution List for ARL-TR-81-19 under Contract N00024-77-C-6200,
Item 0011 (Cont'd)

Copy No.

	Commanding Officer
	Naval Ocean Systems Center
	Department of the Navy
	San Diego, CA 92152
18	Attn: H. Schenck (Code 71)
19	M. Akers (Code 724)
20	H. P. Bucker (Code 5311)

          Office of the Chief of Naval Operations
          The Pentagon
          Washington, DC 20350
21   Attn: J. C. Bertrand

          Office of the Chief of Naval Operations
          Long Range Planning Group
          2000 North Beauregard Street
          Alexandria, VA 22311
22   Attn: CAPT J. R. Seesholtz (Code 00X1)

          Officer-in-Charge
          New London Laboratory
          Naval Underwater Systems Center
          Department of the Navy
          New London, CT 06320
23   Attn: M. B. Moffett (Code 313)
24   W. L. Konrad

          Chief of Naval Research
          Department of the Navy
          Arlington, VA 22217
25   Attn: R. F. Obrochta (Code 464)
26   L. E. Hargrove (Code 421)

          Commander
          Naval Surface Weapons Center
          White Oak Laboratory
          Silver Spring, MD 20910
27   Attn: R. Coffman (Code U20)

          Commander
          Naval Ocean Research and Development Activity
          NSTL Station, MS 39529
28   Attn: A. L. Anderson (Code 320)
29   S. W. Marshall (Code 340)
30   J. Posey (Code 340)

Distribution List for ARL-TR-81-19 under Contract N00024-77-C-6200,
Item 0011 (Cont'd)

Copy No.

Officer-in-Charge
Newport Laboratory
Naval Underwater Systems Center
Newport, RI 02840
31   Attn: K. Kemp, Bldg. 679 (Code 3633)

Commanding Officer
USCG Research and Development Center
Avery Point
Groton, CT 06340
32   Attn: CAPT M. Y. Suzich

33 - 44   Commanding Officer and Director
Defense Technical Information Center
Cameron Station, Building 5
5010 Duke Street
Alexandria, VA 22314

Battelle Memorial Institute
505 King Avenue
Columbus, OH 43201
45   Attn: TACTEC

Applied Research Laboratory
The University of Pennsylvania
P. O. Box 30
State College, PA 16801
46   Attn: F. H. Fenlon
47   G. C. Lauchle

Westinghouse Electric Corporation
P. O. Box 1488
Annapolis, MD 21404
48   Attn: A. Nelkin
49   P. J. Welton

Raytheon Company
Submarine Signal Division
P. O. Box 360
Portsmouth, RI 02871
50   Attn: J. F. Bartram

RAMCOR, Inc.
800 Follin Lane
Vienna, VA 22180
51   Attn: V. J. Lujetic

Copy No.

                System Planning Corporation
                1500 Wilson Blvd.
                Arlington, VA 22209
52   Attn: J. Fagan

                Bolt, Beranek, & Newman, Inc.
                50 Moulton Street
                Cambridge, MA 02138
53   Attn: J. E. Barger
54   F. J. Jackson

                Tracor, Inc.
                6500 Tracor Lane
                Austin, TX 78721
55   Attn: D. F. Rohde

                Radian Corporation
                P. O. Box 9948
                Austin, TX 78766
56   Attn: C. R. Reeves

                General Physics Corporation
                10630 Little Patuxent Parkway
                Columbia, MD 21044
57   Attn: F. Andrews

                Trans World Systems, Inc.
                1311A Dolly Madison Blvd.
                McLean, VA 22101
58   Attn: S. Francis

59   Office of Naval Research
                Resident Representative
                Room 582, Federal Building
                Austin, TX 78701

60   Physical Sciences Group, ARL:UT

6.   Garland R. Barnard, ARL:UT

6.   C. Robert Culbertson, ARL:UT

                Tommy G. Goldsberry, ARL:UT

                            Lamb, ARL:UT

Distribution List for ARL-TR-81-19 under Contract N00024-77-C-6200,
Item 0011 (Cont'd)

Copy No.

  66   Reuben H. Wallace, ARL:UT

  67   Library, ARL:UT

68 - 74   ARL:UT Reserve